ACADÉMIE
DES SCIENCES
INSTITUT DE FRANCE

Comptes Rendus

Géoscience

Sciences de la Planète

Stanislav Jacko, Igor Ďuriška, Juraj Janočko, Roman Farkašovský
and Alexander Dean Thiessen

Structural conditions for relay ramp fault development on the edge of the collision wedge: a case study from the East Slovak Basin

Volume 356 (2024), p. 31-56

Online since: 23 May 2024

https://doi.org/10.5802/crgeos.262

The Comptes Rendus. Géoscience — Sciences de la Planète *are a member of the Mersenne Center for open scientific publishing*
www.centre-mersenne.org — e-ISSN : 1778-7025

ACADÉMIE DES SCIENCES
INSTITUT DE FRANCE

Comptes Rendus. Géoscience — Sciences de la Planète
2024, Vol. 356, p. 31-56
https://doi.org/10.5802/crgeos.262

Research article

Structural conditions for relay ramp fault development on the edge of the collision wedge: a case study from the East Slovak Basin

Stanislav Jacko[a], **Igor Ďuriška**[*,a], **Juraj Janočko**[a], **Roman Farkašovský**[a] **and Alexander Dean Thiessen**[a]

[a] Institute of Geosciences, Faculty of Mining, Ecology, Process Control and Geotechnologies, Technical University of Košice, Park Komenského 15, Košice 040 01, Slovakia

E-mail: igor.duriska@tuke.sk (I. Ďuriška)

Abstract. The Neogene evolution of the Pannonian extensional back-arc basin was associated with the development of transform faults. These faults significantly modified the sedimentary and structural evolution of the basin. The key developmental factors were related to pull forces and to the tilting of the subducted slab. The transitions from upper crustal contraction of upper crustal extension affected the depositional space, which had opened subparallel NW–SE normal faults along the southern contact with the Carpathian collision zone. The entire transition process was controlled by the closing of the rear part of the accretionary space, which changed the dip of the subducted slab. Basin subsidence, which occurred from west to east via N–S steps, generated a system of subparallel-oriented faults, which were connected by relay ramps. The relay ramps had four developmental phases: (a) initial crustal bending, (b) intact ramp formation with structural integrity disturbance, (c) breaching with crustal breakage, and (d) final fault growth. The genesis of the relay ramps of the Eastern Slovak Basin was closely linked to the initial strike-slip movements. The strike-slip movements caused a counterclockwise rotation of the northern edge of the Alpine–Carpathian–Pannonian block. This rotation was later compensated by the tectonic subsidence of the basin, primarily during the Middle Miocene.

Keywords. Relay ramp, Collision wedge, Transform faults, Pannonian basin.

Funding. Slovak Grant Agency VEGA (grants 1/0585/20).

Manuscript received 19 February 2024, revised 9 April 2024, accepted 30 April 2024.

1. Introduction

The Pannonian back-arc extensional basin is associated with the convergence of the Alpine orogenic system during the Upper Cretaceous and Cenozoic [Horváth et al., 2015]. During the Miocene, the Western Carpathians were dominated by oblique intracontinental subduction related to the slab roll-back effect and extruding crustal blocks [Van Gelder et al., 2017]. Studies on recent back-arc areas [Sdrolias and Müller, 2006] describe the unexpected interplay of convergence and extension, and the importance of subduction as the driving mechanism for change. Subduction can occur in various ways, such as in collision-related phenomena, oblique convergence partitioning, and hinge roll-back and/or pull by the subducted slab. Magmatism is not always associated with subduction and depends on the movement of the hinge. Important extensions of the upper plate

*Corresponding author

can be perpendicular and parallel to the length of the subduction zone [Hall, 2002]. The development of back-arc basins is a gradual process that may have many possible controls, such as rifting, back-arc extension, subduction hinge rollback, regional strike-slip faulting, mantle plume activity, basement structural influences, and differential crust–lithosphere stretching [Madon and Watts, 1998, Watcharanantakal and Morley, 2000, Morley, 2001]. In order to understand the basin's structure and geometry, the individual characteristics of the basin must be determined, such as the rate of spreading, asymmetry, magnetic anomaly identifiers, time of activity [Müller et al., 2008], and the inclination of the subducted slab. Back-arc shortening is common [Lallemand et al., 2005] for slabs with a shallow dip of up to 32° (distance of 0–125 km), whereas back-arc spreading commonly occurs in slabs with a steep dip of up to 51° (distance of 0–125 km). Thus, angular differences are key to the dynamics and further development of the basin. Very shallowly inclined plates tend to close the upper part of the crust, whereas steeply inclined slabs spread the upper crust.

The position of the Eastern Slovak Basin (ESB) along the margin of the Pannonian back-arc basin is the result of structural–tectonic evolution, which is related to the tectonic delamination of the back-arc system. During the Middle Miocene, the maximum extension of the Pannonian Basin was approximately 450 km [Ustaszewski et al., 2008]. The structural integrity of the basin was mainly disrupted by the Mid-Hungarian fault zone (MHFZ). The MHFZ originated from a transform fault where the Alpine–Carpathian–Pannonian (ALCAPA) microplate overthrusted the Tisza–Dacia Mega-Unit [Csontos and Nagymarosy, 1998]. The results of this thrusting produced variable amplitudes of extension, ranging from 78–180 km [Ustaszewski et al., 2008]. The ESB structurally opened within a tectonic "triangle" which is bounded by the Darnó fault, the MHFZ, and the Miocene thrust belt. The interaction of individual tectonics in the triangle caused extensional differences in the basin which were related to strike-slip movements and extension, shortening, block rotation [Ratschbacher et al., 1993, Fodor et al., 1999, Márton, 2000, Márton and Fodor, 2003, Csontos and Vörös, 2004, Márton et al., 2007, Tischler et al., 2007], and retreating slabs [Royden, 1988, Wortel and Spakman, 2000, Sperner and The CRC 461 Team, 2005]. The collision between the Eastern Alps/Western Carpathians and the Adriatic Plate (ALCAPA Mega-unit) during the Miocene initiated a period of active subduction, exhumation of the orogenic wedge, basin opening, subsidence, and uplifted the Pannonian Basin [Csontos, 1995, Fodor, 1995, Horváth and Cloetingh, 1996, Bada et al., 2001, Konečný et al., 2002, Horváth et al., 2006, Kováč et al., 1998, 2002, 2016, 2017]. Evidence of Miocene unconformities [e.g., Ginger et al., 1993, Tjia and Liew, 1996, Jardine, 1997, Higgs, 1999] can be correlated to global sea levels [Haq et al., 1987] the geodynamic evolution of the ALCAPA block [Ratschbacher et al., 1991, Oszczypko, 1998, 1999, 2006, Oszczypko and Oszczypko-Clowes, 2006, Oszczypko et al., 2012, Neubauer et al., 2000, Seghedi and Downes, 2011, Van Gelder et al., 2017, Kováč et al., 1997, 2017], and the northeastern escape of the Western Carpathians. These geodynamic changes were primarily related to the pulling forces of the subducted slab, which were affected by asthenolite uplift. The extension between the volcanic arc and the central subsidence region opened new tectonic sub-basins, which were modified by the slab dip. During the back-arc extension period, the sedimentation was controlled by volcanic activity, which indicates different slab dips during the Miocene. The interpreted dips of the subducted slab were approximately 50° and 75° in the Lower Serravallian and the Upper Serravallian, respectively [Lexa and Konečný, 1998].

This study focuses on the development of structural elements near the collision zone of an extensional back-arc basin. These were controlled by tectonic activity related to relay ramp structures, sedimentation and volcanism. Hydrocarbon traps and evaporite deposits are directly linked to these structural elements.

2. Geological and geodynamic relations

During its Miocene evolution, the Alpine–Carpathian orogeny generated different types of deformation structures in its individual palaeogeographic domains. The domains were associated with the subduction of a retreating lithospheric slab [Royden, 1988, Wortel and Spakman, 2000] which lied beneath an upper plate formed by the ALCAPA and Tisza–Dacia Mega-units (Figure 1). The topography of the European Foreland was deformed and modified by

the thrusting of the Outer Western Carpathian (OWC) Flysch Belt [Royden, 1988]. This thrusting reached the Dukla and Silesian units by the Lower Burdigalian (Eggenburgian), approximately 20 MA [Kováč et al., 1998, Oszczypko, 2006]. However, accretion was not identical throughout the seismic profile. The most significant spatial accretion occurred in the fore-arc of the ESB. The structural predisposition enabled the rearrangement of the peripheral units of the Inner Western Carpathians (IWC) during the initial stage of basin formation, and during the development of the Pannonian back-arc basin during the Oligocene [Horváth et al., 2015]. This collision model gradually produced the zonal structure of the Western Carpathians and was associated with several active sedimentation basins. The basin distribution was related to the development of the orogenic system and its transverse division into the fore-arc and back-arc basins [sensu Kováč et al., 2016, 2018]. The Pieniny Klippen Belt (PKB) is a mobile suture zone along the edges of the ALCAPA microplate [Nemčok et al., 2006, Oszczypko, 2006, Ustaszewski et al., 2010, Rauch, 2013, Kováč et al., 2016], along which the Penninic ocean was shortened and engulfed. The PKB helps one understand the overall geodynamic situation in the Western Carpathians. The PKB crustal fragments were thrusted under the former basement, and the flysch belt sediments were thrusted over the foredeep. The tectonic regimes related to the PKB processes were (1) lateral extrusion of the Inner Western Carpathians and the North Pannonian domain (by strike-slip faulting, collision, and orogenic wedge exhumation during mountain development) [e.g., Ratschbacher et al., 1991, Csontos et al., 1992, Kováč et al., 1994, 1997, 1998, 2002, Schmid et al., 2008, Ustaszewski et al., 2008, 2010, Matenco and Andriessen, 2013] and (2) basin opening and crustal subsidence [e.g., Csontos, 1995, Fodor, 1995, Horváth and Cloetingh, 1996, Fodor et al., 1998, 1999, 2005, Bada et al., 2001, 2007, Konečný et al., 2002, Cloetingh et al., 2005, 2006, Horváth et al., 2006, Minár et al., 2011, Matenco and Andriessen, 2013, Kováč et al., 2016, 2018].

The ESB primarily consists of siliciclastic deposits with lesser amounts of evaporites. An important part of the fill is formed by acidic volcanic rocks (the Lower Burdigalian to the Lower Langhian), intermediary volcaniclastics (Langhian to Serravallian), and effusive rocks. The volcanic activity culminated in the Langhian and Serravallian periods. The maximum fill thickness is approximately 9 km, but the data is inconsistent. The depocenters of the basin migrated from the northwest to the southeast. In the northwestern and central parts of the basin, the deposition culminated during the Upper Burdigalian and Lower Serravallian, respectively. The most intensive subsidence in the southeastern basin was recorded during the Middle Serravallian. The basin lies on thin (approximately 27-km-thick) crust that thickens to approximately 30 km towards the north and northwest. The thickness of the lithosphere in the basin is approximately 80 km. The basin contains several gravity anomalies, probably caused by the occurrence of ultrabasic rock bodies. The largest anomalies are located near Sečovce, Zbudza, and in the southwestern part of the Moldava Depression.

The Dynamic opening of the Panonian Basin towards NE was compensated by perpendicular N–S oriented faults. These faults were concentrated in the eastern part of the ESB and compensated the basin's rapid subsidence towards southeast.

The Slánske Mts. volcanic chain, which is also oriented N–S, divides this set of faults (such as the Hornád, Albinov, and Ondava fault). The volcanic chain also separates the ESB into the eastern (Košice) and western (Trebišov) depressions.

It therefore can be assumed that a transform fault exists along the volcanic chain which was a channel for Miocene intermediate volcanism. The interpretation of deep seismic profiles (705/92, 706/92, Figure 2) confirmed the existence of a system of normal step faults ranging from the western margin of the ESB up to the volcanic chain. In this 15 km wide ranging area, we can observe (as in the example of the Middle Triassic Dolomites) tectonic subsidence up to 2500 m in depth.

East of the volcanic chain there are dolomites buried at a depth of 4000 m (583/85, Figure 2). The depth at which the dolomites occur along the western and eastern edge of the volcanic chain differs significantly. For this reason, it can be assumed that there is a transform fault running along the length of the volcanic chain, which would be tied to the abovementioned subparalell N–S faults. The faults mark the tectonic boundaries between the Miocene ESB and the pre-Miocene IWC units, as well as several depositional subbasins which developed towards the east (Košice, Vranov, and Michalovce). Additionally,

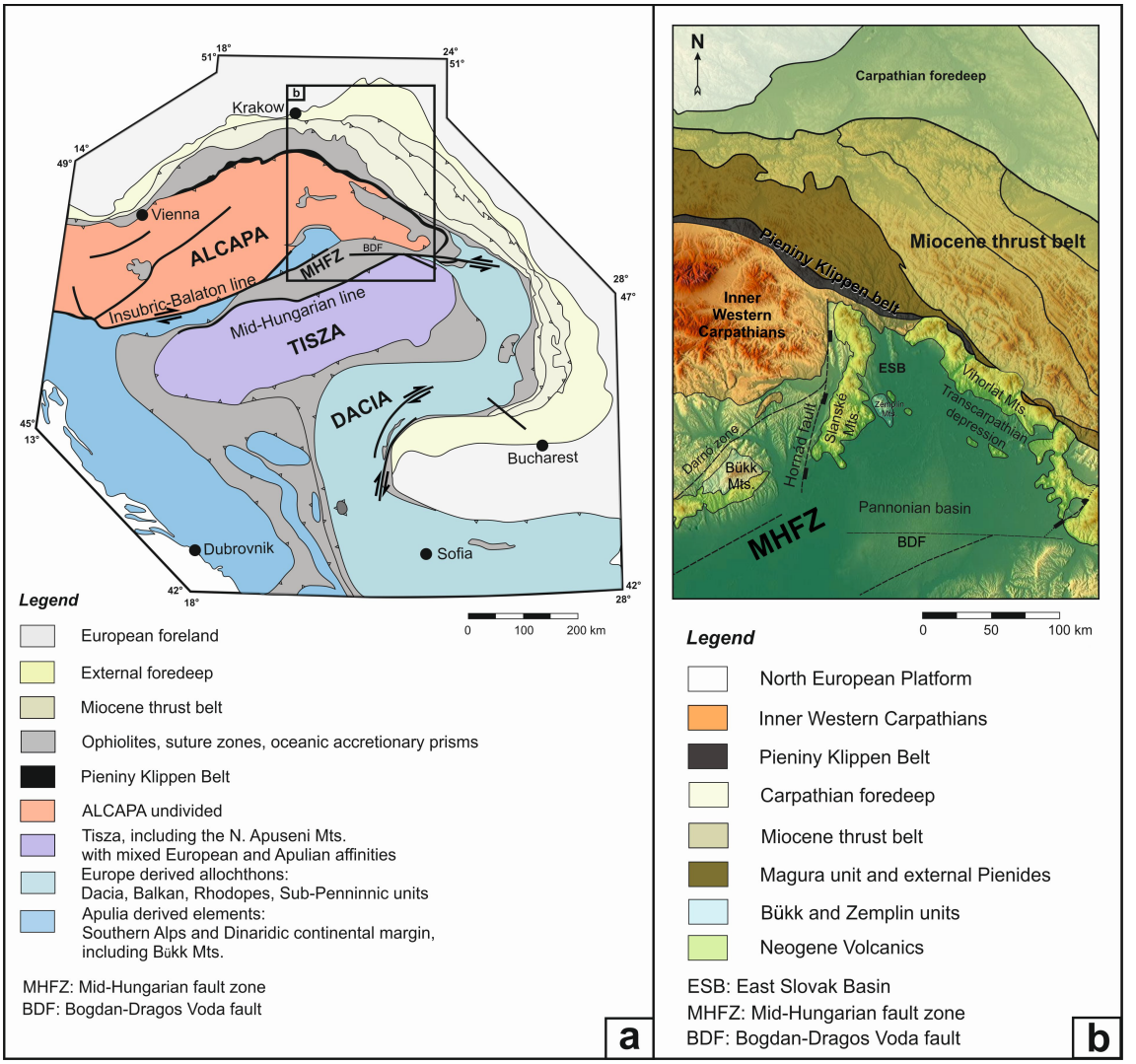

Figure 1. (a) The opening of the Pannonian back-arc basin is related to the tectonic evolution of the microplates, which are bounded by deep core faults. (b) The Eastern Slovak Basin is a northern peripheral basin and part of the Transcarpathian depression situated between the southern edge of the collision wedge, the Mid-Hungarian fault zone, and the Hornád fault/linked with the Darnó fault system in the west [modified after Ustaszewski et al., 2008, Márton et al., 2007].

the subducted slab was broken in this zone, and the lithospheric plate became more inclined [Csontos, 1995]. These changes were controlled by increased sedimentation in the eastern areas.

3. Methodology

Relay ramp research was carried out using datasets collected from surface analysis of Eastern Slovak Basin deposits. The datasets also used the facies analysis of drill cores, the analysis of electricity well logs, seismic data interpretations, seismostratigraphic analysis, structural and geological research and modelling. Additionally Spontaneous Potential (SP) responses were used and were compared to seismic reflectors [Jacko in Žec et al., 1997, pp. 1–254; Jacko in Hrušecký et al., 2000; Jacko in Janočko et al., 2006; Jacko in Sály et al., 2006,

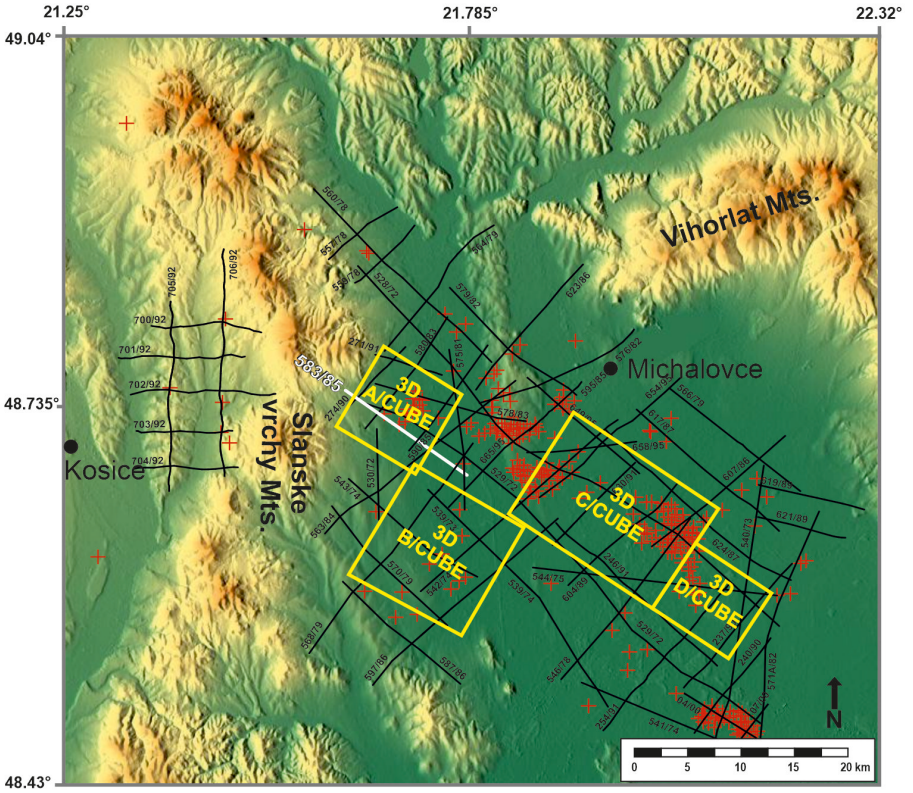

Figure 2. Spatial distribution of the 2D seismic cross-sections, 3D seismic cubes (A/cube—locality Višňov, B/cube—locality Trebišov, C/cube—locality Senné-Stretava, D/cube—locality Pavlovce) and exploration wells, realized during hydrocarbon exploration and excavation by the Nafta Oil Company in the Eastern Slovak Basin.

Pachocka et al., 2010, 62 p; Jacko in Fričovský et al., 2012, Jacko et al., 2014, 2021a].

3.1. *Seismic analysis and modelling*

Hydrocarbon and (to a lesser extent) geothermal exploration during the last few decades have prompted several drilling campaigns accompanied by geophysical, structural, sedimentological, and geochemical exploration. In this study, the results from 341 boreholes were added to the database for further evaluation and modelling using Schlumberger Petrel v.2010.1 software and Golden Software Surfer 12. Geophysical campaigns from ESB Basin included 2D and 3D seismic exploration which covered an area of 2000 km^2. We used 56 2D cross-sections (Figure 2) with varying orientations (mostly NW–SE; with fewer NE–SW, N–S, and W–E campaigns from 1974–2000; with a total length of 940 km). This study used four 3D seismic cubes covering an area of 450 km^2: 3D Višňov (8 × 8 km), 3D Trebišov (12 × 12 km), 3D Senné-Stretava (17 × 11 km), and 3D Pavlovce (8 × 7 km).

The seismic cross-section processing yield results with reversed polarity [Brown, 1991]. Although the vertical scales of seismic sections are in TWT, key observations (e.g., sediment thickness and fault offsets) in the article were calculated in meters based on the correlation of SP responses (SP tie) from wells in the study area. The SP ties should be correct; however, inaccuracies may occur due to the scarcity of check shots in the area. The age of the mapped seismic horizons were identified based on 341 wells localized inside the studied area.

3.2. *Structural analysis*

The deep seismic analyses were compared to the results of the structural analysis. Temporal, spatial

and structural relationships were analysed and correlated with each other. Structural research was carried out in a wide area of the ESB. This includes several lithotectonic units, such as the Veporic Unit (crystalline Paleozoic basement with Mesozoic cover), the Fatric Unit (Mesozoic carbonates), the Inner Carpathian Paleogene Basin sediments (Eocene-Oligocene/Eger), the Pieniny Klippen Belt (Jurassic—Cretaceous sediments), the Carpathian Flysch Belt (Paleogene sediments), and the ESB (Eggenburgian–Pannonian sediments and volcanic rocks). Structural analysis and paleostress calculations were completed using TectonicsFP software.

3.3. *Relay ramps*

The relay ramps are typical structural patterns that involve extensional tectonics and that control deposition and sedimentary fill [Corfield and Sharp, 2000, Gawthorpe and Leeder, 2000, Gawthorpe et al., 1997, Hamblin, 1965, Rotevatn and Jackson, 2014, Schlische, 1995, Sharp et al., 2000, Withjack et al., 2002, Serck and Braathen, 2018]. The development of relay ramp structures has been studied in rift basins, where three stages of development have been identified: (a) fault initiation, (b) fault intersection and linkage, and (c) through-going fault stage [Cowie et al., 2000, Gawthorpe and Leeder, 2000]. The basic geometric characteristics [e.g. Fossen and Rotevatn, 2016] are based on comparisons of the fault length (fault overlap), the relay ramp width (fault separation), and the relay ramp dip [Soliva and Benedicto, 2004, Huggins et al., 1995, Xu et al., 2011, Rotevatn and Bastesen, 2012, Giba et al., 2012, Bastesen and Rotevatn, 2012]. Soliva and Benedicto [2004] suggested a breaching criterion (c^*) based on the relationship between the relay displacement (D, the sum of the fault displacement) and the relay width (fault separation, S) of the form $D = c^* S$, where c^* varies from 1 ($D = S$) to 0.27 ($D = 0.27S$) for relays that show evidence of incipient breaching.

4. Results

The results of structural research have confirmed that the development of ramp structures in the depositional space of the ESB depends on the initial processes. These initial processes "prepared" the ramps for their subsequent formation and development. In general, a ramp structure development is associated with crustal extension. Paradoxically, in the initial deformation stage of the ESB, the crust was exposed to shortening in transpressional deformation conditions.

4.1. *Basin opening on the edge of the collision zone (initial stage), Wrench basins*

The migration of the subduction boundary of the European platform toward east initiated a number of shortening processes which were compensated by thrusting in the accretionary zone of the OWC [e.g. Kováč et al., 1998, Oszczypko, 2006], during the Lower Burdigalian (Eggenburgian). The major regional consequences of extreme shortening in the accretionary wedge included: (a) inclination changes of the subducted slab, (b) steepening of the wedge-top basement, (c) flysch belt space reduction compensated by overthrust and crustal bending in the foredeep, (d) south-vergent thrusts of pre-Miocene units situated in the frontal part of the ESB and the Pieniny Klippen Belt, (e) exhumation of the Pieninic nappes, (f) double or triple (Figure 3) the tectonic thickening of the pre-Miocene IWC deposits, and (g) strike-shear movements that compensated shortening activity [0, 0, 0].

Collisional processes along the boundary between the ESB and the Pienniny Klippen Belt were compensated by dextral transpression which formed a flower structure and splay wrench basins (Figure 4). Simultaneously a number of south-vergent isoclinal fold structures formed in Paleogene/Lower Miocene sediments. These have fold axes that are oriented in a WNW–ESE and a E–W direction. The folds are associated with the thrusting and tectonic thickening of the basal Paleogene sediments, which overthrust the Mesozoic Humenne Unit.

This deformation stage initiated a sedimentary hiatus in the ESB during the Middle Burdigalian. Additionally, Riedel shears formed, such as the NNE–SSW sinistral and NNW–SSE. These have been observed in Mesozoic carbonates of the Humenné Unit along the NE edge of the ESB. This entire structure was fixed in place by the overlying Serravallian (Upper Badanian–Sarmatian) volcanics.

In the vertical log it is possible to observe the following sedimentary facies:

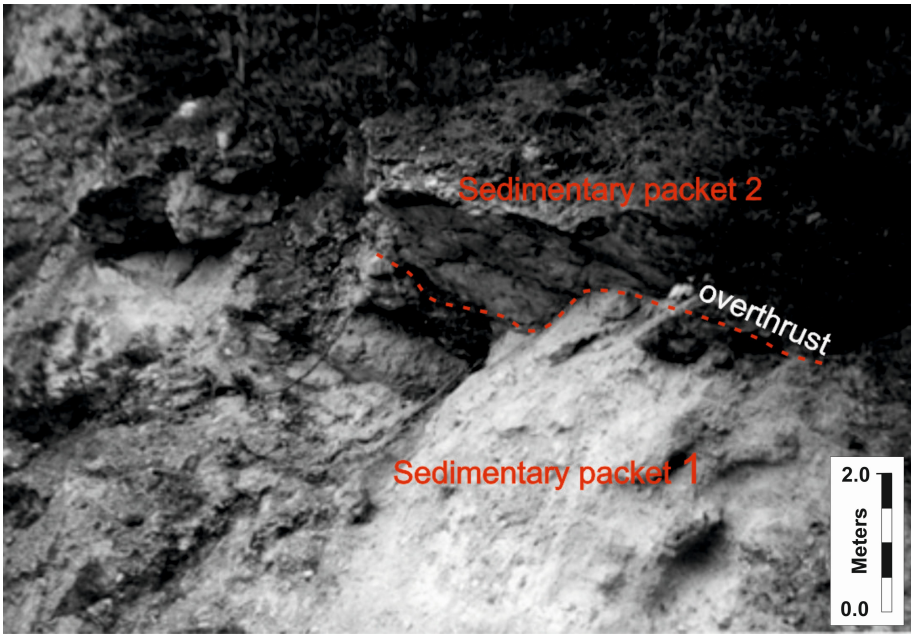

Figure 3. Reverse south-vergent overthrusts along the edge the collision zone (GPS coordinates of the location: 48°54′4.10″N 21°55′44.97″E) of the Pieniny Klippen Belt, which enabled the movement and displacement of the peripheral units (Iňačovce–Kritchevo unit, Humenné Mesozoic unit, Inner Carpathian Paleogene unit) of the Western Carpathians towards South. Tectonic thickening of the basal conglomerates was confirmed by nummulite zones which occur in all tectonic packets.

- Clast-supported, massive, and rarely positively graded conglomerates.
- Matrix-supported, massive, and inversely graded conglomerates with high matrix content.
- Clast- to matrix-supported, parallel-laminated pebbles with a mean clast size of 0.5 cm. The thickness of the laminae is determined by the clast size and the lamination is formed by alternating coarse and thin laminae, which consist of larger (maximum 1 cm) and smaller clasts.
- Medium-grained sand with scattered granules.
- Horizontally laminated fine-grained, muscovitic, dark-brown sand and silt.
- Planar, cross-stratified, medium-grained sandstone with occasional granules. Granules are arranged along the laminae and emphasize cross-stratification. The mean dip of planar cross strata is toward the NNW. The base and top of the beds are sharp, the bed thickness is about 15 cm. This facies usually fills small erosional scours, or it laterally passes into massive sandstones of facies 4.
- Thin layers of conglomerate are represented by well-rounded clasts with a mean diameter of 6 cm, which mainly comprise of one-clast thick beds.

Sedimentary facies described in the vertical log (Figure 4) are interpreted as sediments deposited in an environment containing delta fans or steeply inclined ramps. Shortening space in the collision zone (Figures 3, 4) caused crustal loading. This loading was compensated by the occurrence of dominant depressions in the N–S direction, which occurred after the sedimentary hiatus. The depressions developed from the edge towards the center of the basin. A new deposition center subsequently opened during the Karpathian period [Vass et al., 2000]. The sedimentary fill occurred nearly throughout the entire basin and corresponds to the extension of the Pannonian Basin.

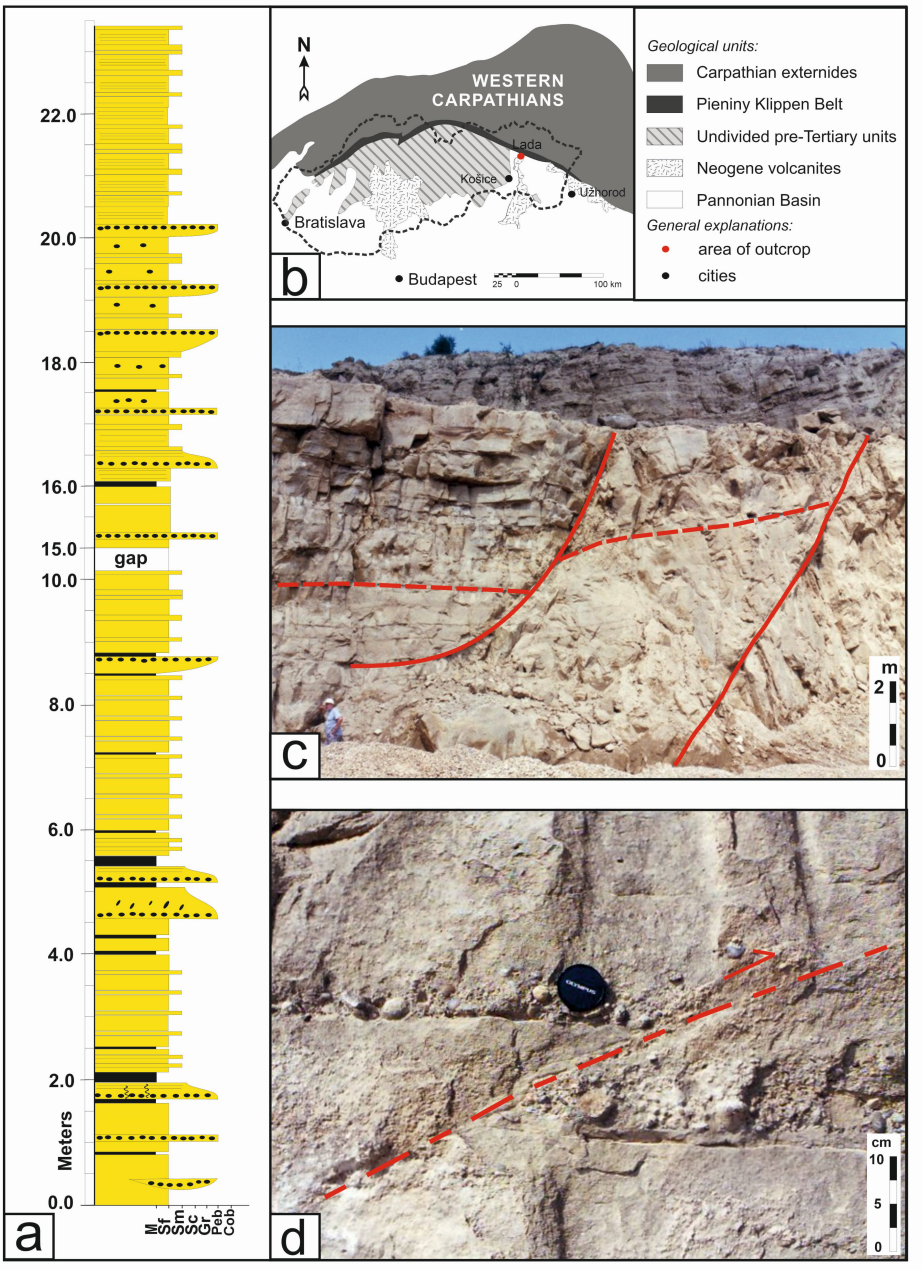

Figure 4. (a) The sedimentary log from the splay wrench basin (approx. 500 × 250 m) at the northern margin of the studied area in the ESB (GPS coordinates of the location: 49°03′18.2″N 21°22′13.5″E). The vertical lithological logs documents the dynamics of the opening, deposition, and closure stages of the basin. (b) The location of studied outcrop. (c) Massive fine to medium-grained sandstones with a monoclinic inclination of 20° to 35° to the northeast with well-developed foreset beds. Sediments are segmented by listric and planar normal faults with a NNW–NNE direction, and a steep dip towards WNW. (d) Cemented syn-sedimentary thrusts which developed before the diagenesis of the sediment. The sandstone boudins in these claystones are parallel to thrust faults. Middle Burdigalian shortening on the northern edge is related to the uplift and sedimentary hiatus in the ESB.

4.2. *Basin differentiation linked to relay ramp development*

Structural changes in the Middle Miocene were related to modified geodynamic conditions in the Pannonian Basin and were reflected in all major crust fault lines, such as the MHFZ (including the Darnó fault system, where the ALCAPA overthrusts the Tisza–Dacia Mega-unit) [Csontos and Nagymarosy, 1998]. The maximum basin spreading escalated the crust delamination process, which created asymmetrically arranged relief. The Burdigalian evolution of the ESB lacks structural field data. Well and seismic sedimentary data shows us that the basin depocenter was located in the axial part of the basin. The subsidence was controlled by NE–SW extension along dextral oblique normal NW–SE faults, when the northern edge of the basin was slightly uplifted. The sedimentary fill at the base of the Burdigalian rocks begins with well sorted clasts and sporadic andesite fragments. The clastic sediments are covered by a lens shaped halite body 60–80 m thick and 3 km long.

The advancing uplift in the north caused sea level regression, which subsequently lagunar sedimentation up to 300 m thick. The evaporites are tied to those sub-basins which have their axes oriented N–S (Figure 5). The step-arranged sub-basins gradually moved away from the collision zone (sub-basin A: 7 km, sub-basin B: 10 km, sub-basin C: 23 km). The delamination of the crust (from the west to the east) was controlled by subparallel faults systems, and relay ramps connected to them. The axes of the main distribution channels are oriented parallel to the direction of the fault networks and change position depending on the amount of increasing subsidence. The most striking changes are connected to breaching, which generated perpendicular NE–SW extensional faults, that were later used as pathways for fluid migration [Jacko et al., 2021a]. This is supported by current geothermal exploration in the area.

4.3. *Relay ramp development*

The relay ramps were studied in detail east of the Slanske Mts. volcanic chain (Figures 6, 12). The ramps are linked to the Albinov fault system (AFS). The faults footwall was formed in the N–S direction with a medium to steep inclination towards the east. The Podslanský foothills were formed parallel to the fault as a product of Miocene volcanism, which was associated with the ESB development. AFS epizonal (multi-genetic) development continues into the present, as demonstrated by earthquake epicenters with macroseismic effects ranging from 3 to 5 MSK-64. The stratigraphic record along the AFS is formed by the buried Iňačovce–Kritchevo Unit which are overlain by Neogene sediments of the ESB. The number of 3D seismic surveys were implemented in the area to methodically solve the problem of how relay ramp systems were formed.

4.3.1. *Initial stage—crustal bending*

The formation of the relay ramp fault system in the early stages of back-arc extension was controlled by the tectonic transition at the basins margin, which was a collision zone during the and Lower Serravallian (Upper Badenian). The deltaic depositional systems architecture with its distributional channels suggests there was an increase in subsidence at the southern edge of the AFS. This subsidence would have been related to the initial formation of the half-graben structures at the southern margin of the basin.

Most coarse-grained material was progressively deposited on the western edge (later inboard fault) of the future AFS environment from the NNW to the S. The sigmoidal curvature of the depositional system (Figure 10) indicates a change in slab inclination with subsidence towards the edge of the plate, that had not yet been tectonically ruptured. The presence of separate individual segments [Trudgill and Cartwright, 1994, Walsh et al., 2003, Fossen and Rotevatn, 2016] and embryonic faults was not confirmed in the initial stage [e.g. Cowie et al., 2000, Soliva and Schultz, 2008]. The material was homogeneously deformed [McClay and Ellis, 1987, Vendeville and Cobbold, 1988, Wu et al., 2015] by a flexural bend in the upper part of the crust, which compensated for the massive subsidence that occurred at the southern margin of the basin.

As can be seen in Figure 7, the subsidence created a structural depression in the N–S direction that is well-documented by the third distributary channel at the eastern margin of the ESB. This distributary channel has a general NE–SW orientation and shows signs of eastward migration (Figure 7).

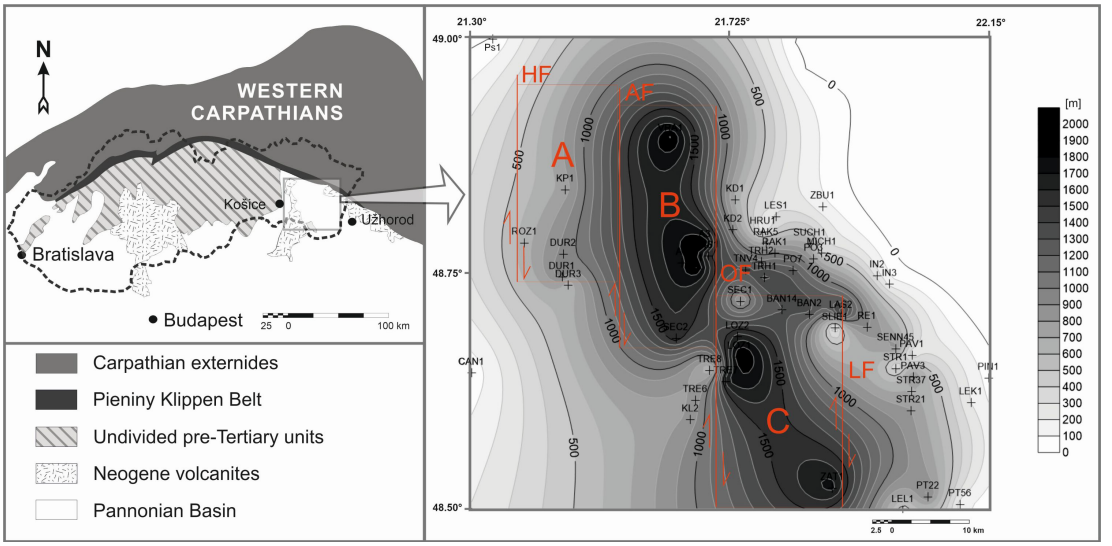

Figure 5. The arrangement of the elongated subbasins is related to the bookshelf effect, the axially oriented distribution of sediments, and strike-slip/normal fault development during the and Lower Serravallian (Upper Badenian). The development of sub-basins was gradual from West to East (from the oldest A to B and youngest C). The offset of the sub-basins is related to the dominant tectonics of N–S direction. Sub-basin C, (the youngest) is already under the partial influence of the NW–SE system, which began to dominate from the Middle Serravallian (Lower Sarmatian). A—Košice depression, bordered in the West by the Hornád fault system (HF) and in the East by the neovolcanic roks of the Slanské vrchy. B—Vranov depression is bounded in the West by the Albinov fault (AF) and in the East by the Ondava fault (OF). C—Sliepkovce depression is tectonically bounded by the Ondava fault (OF) and the Laborec fault (LF).

4.3.2. *Intact ramp formation—crust rupture*

The dominant extension continued until the end of the Lower Serravallian, where it fractured the upper crust through flexural bending, and formed a fault system [Vass et al., 2000]. During this period, en-echelon subparallel faults were formed, that consisted of individually growing faults. We assume that this phase was associated with the rupturing crust and was isostatically compensated for the "unnatural" crustal bending. This led to the retreat of the distribution channel to the north. The vertical displacement of the fault system reached 450 m along the southern margin. The aforementioned events were likely accompanied by seismic shocks [Janočko, 1996, Řeřicha, 1992]. A narrow, dynamically meandering deposition channel with a southward inclination opened parallel to the fault system. Higher seismic amplitude at the Lower Serravallian structural horizon (Figure 8) documents the distributary channel development. Sea regression and sedimentation occurred in a dynamic delta environment [Vass et al., 2000]. Dynamic subsidence increased the ESB extension, and deposits of coarse-grained clastic material transported by deltaic systems [Janočko, 1990, Reed et al., 1992, Řeřicha, 1992, Janočko, 1993, 1996, Hlavatá and Kováč, 2010] accumulated in the marginal N, NW, and W sides of the basin.

Sediments deposited in the mouth bars of the terminal parts of the deltaic distributional channels allowed the progradation of coarse-grained sand bodies from the margin of the basin from NE and N to the SW and S. The western margin of the Albinov fault displays a similar situation. The increasing subsidence gradually initiated antithetical parallel-oriented faults, which completed the relay ramp system. The faults are most visible in the northern part of the basin, where four such identified systems reached developmental stage B [sensu Peacock and Sanderson, 1991, 1994] without the occurrence of a fault breach (Figure 8).

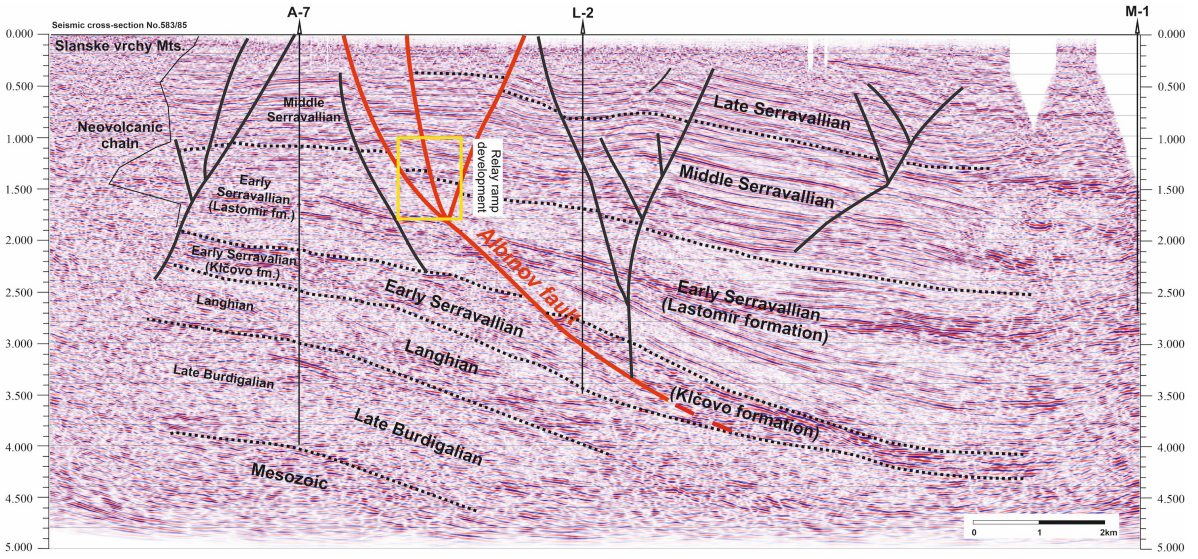

Figure 6. The Albinov fault system (AFS) represents a juxtaposition zone between the Iňačovce–Kritchevo and the Veporic basement (under Karpathian sediments) units. The AFS is a shear-zone which compensated the counter-clockwise basin movements and oblique normal fault with high subsidence during the Langhian and Serravallian sedimentation. The result of the polystage evolution was the formation of the flower structure, joined with the listric shape of the fault.

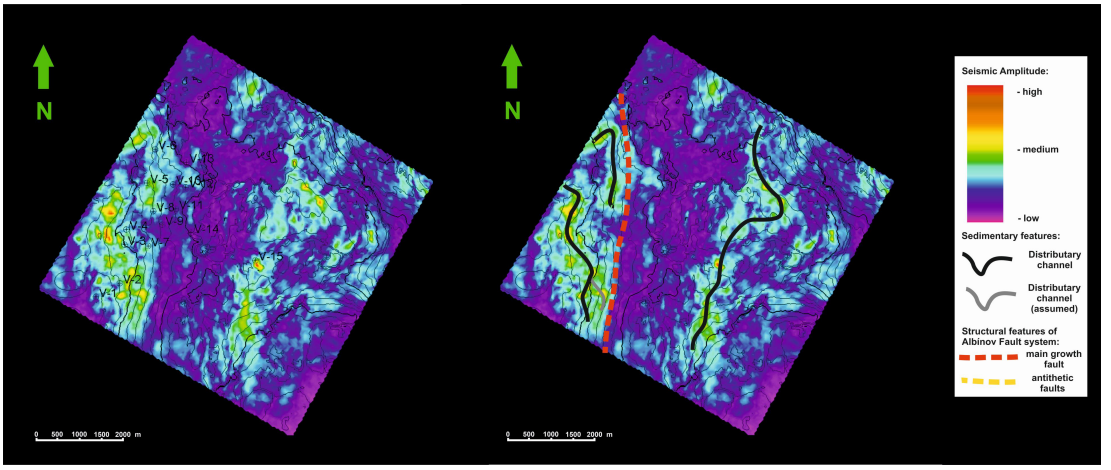

Figure 7. Initial stage: (left) The Upper Badenian (Lower Serravallian) base horizon of the western margin of the ESB with no signs of tectonic rupture. (Right) Orientation of the distributional channels corresponding to the distribution of coarser sedimentary material which was distributed from the north to the south.

4.3.3. *Relay ramp breaching*

AFS activity in the Middle Serravallian was sufficient to interconnect individual segments. The fault direction was generally N–S, and the normal throw was compensated by antithetically and synthetically oriented faults. The newly created ramp captured deposits in the interdistributary area. This

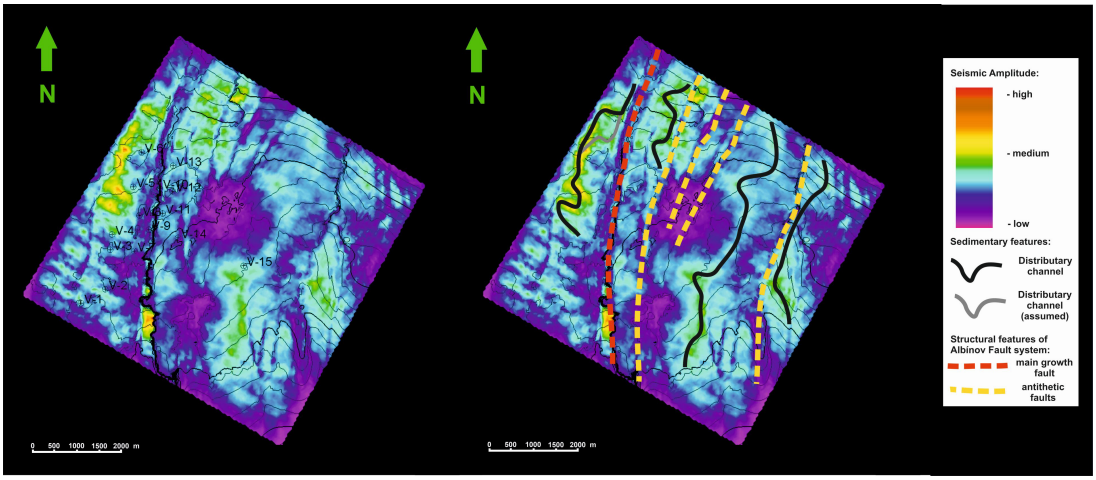

Figure 8. The structural surface of the Upper Badenian (Lower Serravallian) horizon points to the tectonic activity of the AFS and the formation of en-échelon subparallel fault. Already in this period, the highest tectonic block was formed in the western part of the depicted surface. The fault drops to a maximum of 450 m southward.

development coincides very well with the tectonic development of the ESB, which contains documented medium steep uplifts at the northern margin of the basin with a collision edge. The uplifts primarily compensated subsidence in the central area and the opposite margin of the basin, where the declines were dominated by NW–SE-oriented planar and listric faults (documented in 5 other locations). Well logs located on the AFS ramp indicate lateral migration of the distribution channels, which were probably affected by pulse ramp movements. This indicates breaching between the inboard and outboard faults (Figure 9).

4.3.4. *Geometry finalization*

The geometry of the Albinov relay-ramp structures reached its definitive and final form at the end of the Middle Serravallian. Normal faulting determined surface morphology, sedimentary routing, and stacking patterns [Corfield and Sharp, 2000, Rotevatn and Jackson, 2014, Serck and Braathen, 2018]. The 3D seismic cross-section cube identified an expansion of the faults related to planar surface breaching faults (Figure 10). The AFS is a planar structure with conjugated-oriented faults. The maximum throw between the footwall and the hanging wall was approximately 1100 m, and the hanging wall horizons created wedge-shaped sedimentary packages [sensu Serck and Braathen, 2018]. The footwall in the cross-section, parallel with the fault, is characterized by alternating high, medium, and low amplitudes that are related to dynamic conditions present during deposition (Figure 11). The interpretation of the depositional environment indicates an environment which was influenced by deepening sedimentary basin conditions, during a period of tectonic subsidence.

4.4. *Relay ramp geometrical classification*

The relay ramp geometric structure classification is primarily based on half-graben geometry [according to Morley et al., 1990, Morley, 1995]. The comparison and application of the methods is limited by the technical documentation, which is related to:

- The detail and quality of processing (geophysical or surface data).
- The rate of structural and sedimentary basin modification or revisions.
- Erosion (especially of surface sources).
- Research horizons (that must correspond to one-time record).
- The time to depth conversion.

During the ESB development, the area of subsidence migrated from the NW to the SE. Changes

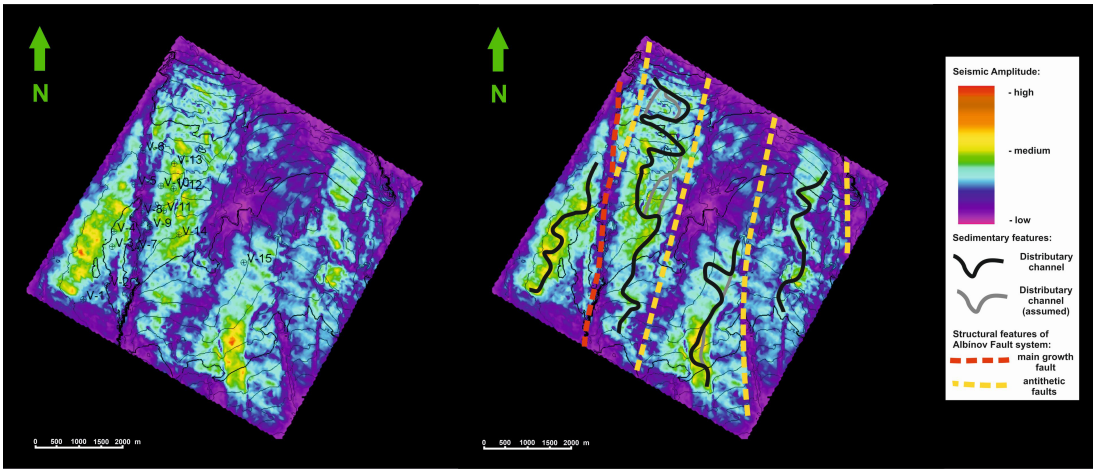

Figure 9. The structural surface of the base of Middle Serravallian (Lower Sarmatian) with the interpretation of the distribution channels, with the deposition of sediments from the N and NE to the S and SW. The sandiest parts are located West of the AFS on the ramp. The longest distribution channel is situated on the ramp, which is bounded by the antithetically oriented fault.

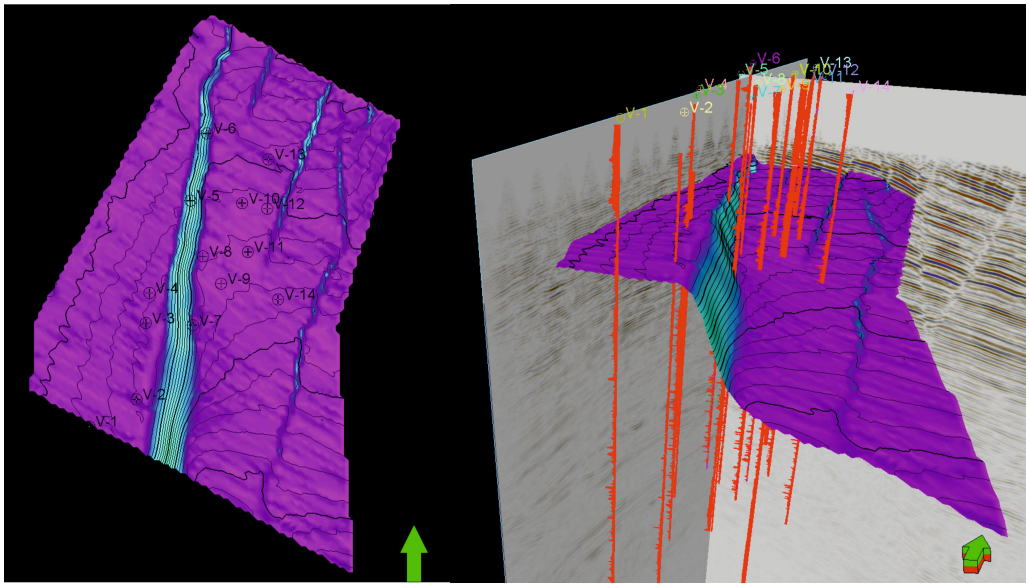

Figure 10. 2D–3D spatial and geometric view of the fault relay structure of the Albinov fault system.

in the inclination of the subducted slab, and fault-related processes at the MHFZ caused: accelerated tectonic activity, increased heat flow and initiated tectonically controlled rapid subsidence. The response to this crustal effect was the evolution of concave structures that predominantly compensated for the south-oriented extension. In these geodynamic conditions, dominant half-graben type faults were compensated by antithetically oriented growth faults. The growth faults locally changed the deposition trajectories.

Curved, synthetically oriented faults with an initial N–S direction (Figure 12) dominated the structural system. The initial WNW–ESE and subsequent

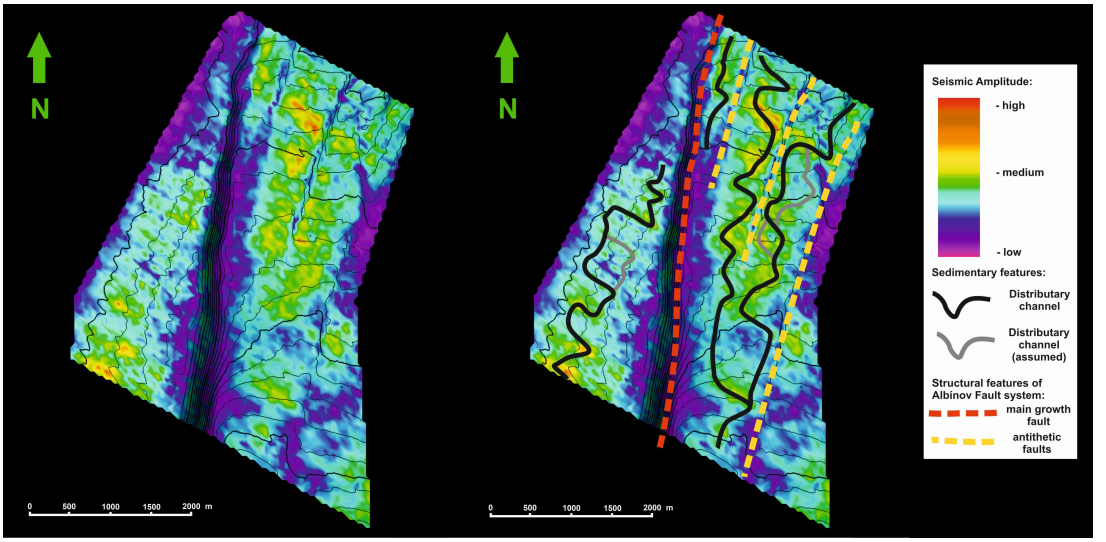

Figure 11. The structural surface horizon of the Lower Sarmatian (Middle Serravallian) period (on the left) with the relay ramp structure and its four interpreted distributional channels (on the right) [sensu Pickering et al., 2014, Shepherd, 2009]. The channels reveal migration and avulsion. High amplitudes—red, yellow, and yellow-green document the sandiness of the environment.

NE–SW extensional regimes were gradually interconnected by the synthetically and antithetically oriented faults. These were later transformed into transtensional faults that generated the relay ramp geometry.

The Middle Serravallian structural surface was geometrically classified (Table 1). The seismic cross-section was easily interpreted due to clear sedimentary and tectonic structures, a sufficient dataset source, and the absence of erosional surfaces. The individual segments were geometrically analysed using a multi-criteria approach. The variable width, length, and slope values of the ramp segments do not affect the width or opening of the fault structure. The inclination of the ramp varied from 2°–4°. Values from 5°–9.8° were deviations from the average. All the surplus values were concentrated in a broad zone, in which the structural links between the N–S and NW–SE systems were most likely compensational. The thickness model of Upper Serravallian deposits correlates very well with the before mentioned zone. However, the relationship between ramp structures and the primary "parent" fault zone was confirmed. The ramp segments showed increasing slope values with increasing distance from the primary fault. Paradoxically, the width-to-length ratio is close to 1.

We used the results of the geometric analysis to conclude that relay ramp development depends on the following:

- The orientations of potential ramp structures in relation to the paleo-stress field distribution.
- The positions of particular faults in the overall structure.
- The position of the ramp in reference to the primary subduction area, where the marginal structures show inclination differences (this factor did not affect the width of the fault surface or the slope).
- A wide range of structural zones correlated to heat flow distribution.

The asymmetric arrangement of structural elements significantly limits the range of hydrocarbon deposits:

- Hydrocarbon structural traps are tectonically limited by a system of listric fault structures, on which hydrocarbon migration also occurs.
- Structural zonality is thus an important factor for understanding the distribution of underground deposits, whether hydrocarbons or geothermal energy sources.

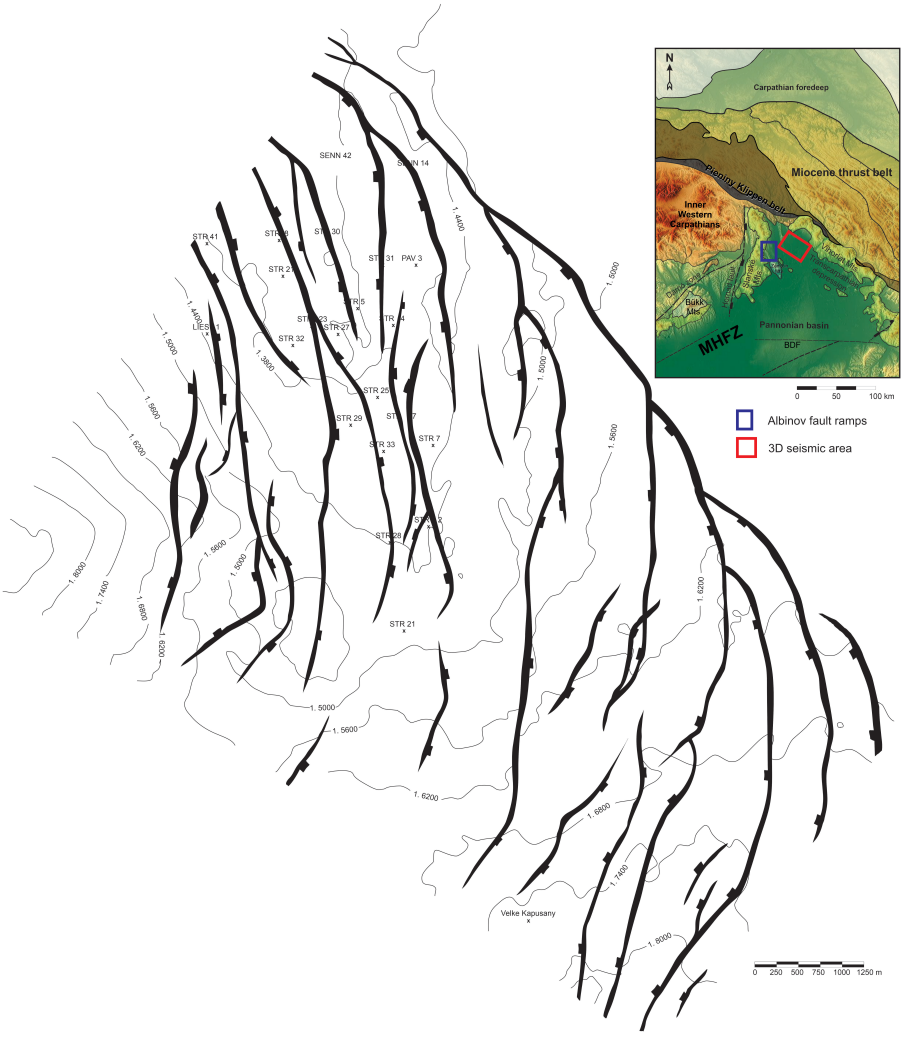

Figure 12. The rapid subsidence along the northern edge (red frame) of the Eastern Slovak basin was compensated by relay ramp growth faults. The irregular fault geometry which increases with distance from the major fault can be seen on the isohypse near the Middle Serravallian (Lower Sarmatian) sedimentary horizon [modified after Sály et al., 2006].

4.4.1. *Structural observations*

By observing the geological structural framework, it is evident that there is a relationship between an increasingly more dynamic upper crust and increasing internal deformation and slab inclination. This is connected to the formation of multiple faults and fractures, which are dependent on several rheological and mechanical layer properties. In general, it was presumed that the development of the ESB (Figure 13) was primarily linked to the development of fault structures NW–SE parallel to the Pieniny Klippen Belt [Jacko et al., 2021b]. However, the dominance of this NW–SE system only starts in the Miocene because of rapid subsidence. This was supported by crustal heating, and associated volcanism. The subsidence transported the main depression towards SE. The influence of the Hornád Fault system (Figure 13) along the western margin of the ESB decreases, while the influence of subsidence and antithetical shear structures (such as horse tail structures and later relay ramps) increases. The formation

Table 1. Geometry patterns measured from each fault limbs

Fault No.	Geometry	Shape	Width (meters)	Length (meters)	Fault heave (degrees)	Height/ length	Inclination	
							Degree	Dip to ramp orientation
1	Synthetic	Curve	500	1600	50	1:21.4	2.7	Parallel
2	Synthetic	Curve	1025	3600	70	1:17.1	3.3	Parallel
2*	Conjugate	Linear	600–1200	4125	75–50	1:15	3.8	Parallel
3	Synthetic	Curve	950	3625	50	1:22.7	2.5	Parallel
3*	Conjugate	Curve	600–1125	2625	45–60	1:14.6	3.9	Parallel
4	Synthetic	Curve	960	2125	40	1:19.3	3	Parallel
5	Synthetic	Curve	625	4475	75	1:26	2.2	Parallel
6	Synthetic	Curve	750	4750	75	1:8.3	6.8	Perpendicular
7	Synthetic	Curve	750	2700	50	1:5.8	9.8	Perpendicular
6*, 7*	Conjugate	Curve	800–1500	4750	40	1:10 1:11.4	5.7 5	Perpendicular parallel
8	Conjugate	Linear	780–1450	6500	45	1:24.2	2.4	Parallel

of relay ramps in the ESB is therefore connected to transform faults that are parallel to the Hornád fault system. These faults also restricted the CCW rotation of the NE edge of the ALCAPA plate. Later, during the middle Miocene, they compensated the tectonic subsidence of the basin in the SE.

If there is connection between the slab's inclination and the strained state of the upper crust, then it is evident that the Hornád fault system is a genetically transform fault, with a high degree of heat flow. Geothermal activity reveals a clear zonation trending E–W and N—which is a result of a combination of structural (thickness and spatial distribution of horizons), lithological (variations in carbonates, siliciclastics, evaporites, andezite tuffites) and geothermal features (approximated thermal conductivity, basal heat flow densities, radiogenic heat production, geothermic gradient and basal temperatures).

5. Discussion

5.1. *Volcanism*

Syndeposition volcanic and intrusive activity (Figure 14) were the main signs that accompanied the Neogene evolution of the Pannonian basin and its peripheral areas. They are characterized by their spatial distribution, and their relationships to tectonic phenomena such as subduction, slab breakoff, tectonics and the block rotations of microplate segments. Volcanism (from 21 to 0.01 Ma [Pécskay et al., 2006]) in this area is generally related to the subduction and collision of that crust which underlies the former Outer Carpathian flysch basins.

The ESB's centers of volcanism are concentrated in three areas [Lexa and Konečný, 1998]; the activity of which moved from west to east over time. The first center was the westernmost, Slanske Mts. volcanic chain. This chain is parallel with the N–S Hornád fault system. A system of nine linearly arranged pyroxene andesite stratovolcanoes follow the same path. The volcanoes decrease in age as one moves from north to south, with Middle Burdigalian stratovolcanoes in the north, and Tortonian volcanoes in the south. Similarly, it is possible to see environmental and geological changes between the north and south regions. In the north the volcanoes are formed by diorite porphyre stocks with epithermal mineralization. The meridional region is dominated by shallow marine conditions with hydromagmatic pyroclastic deposits [Lexa et al., 2010]. The second center is located along the southern edge of ESB and is rimmed by andesite volcanic cones and effusive complexes. Volcanic activity started at 14.5 Ma in a shallow marine environment. This area is dominated by effusive andesite with complexes which contain rhyollitic pumiceous tuff horizons, hyaloclastic breccias, and hydromagmatic products. Later, the Tortonian period (9.5 Ma) was related to the formation of large andesite stratovolcanoes. The third and final center of volcanism is the northern edge of ESB and partial accretionary wedge. The edge

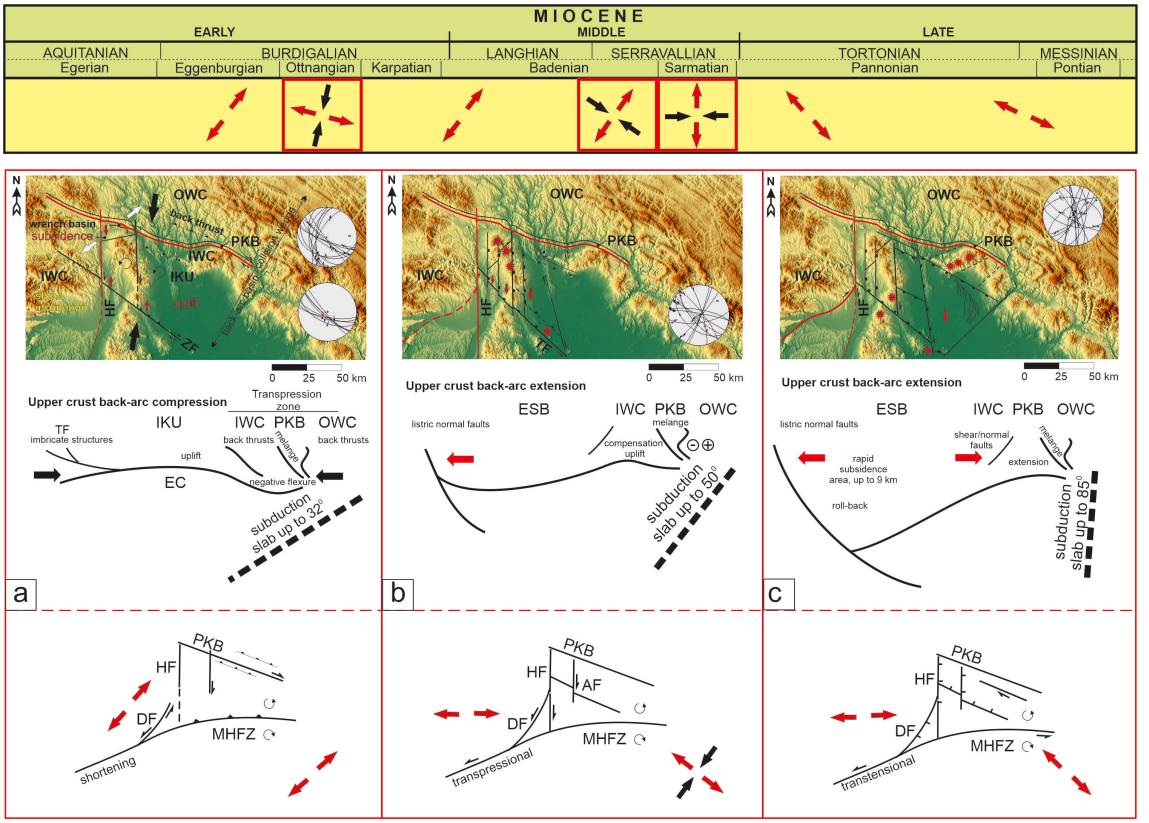

Figure 13. The tectonic evolution of relay ramps in the ESB is connected with the developmental phases of the Mid-Hungarian Fault Zone and the back-arc basins development [according to Csontos and Nagymarosy, 1998, Márton et al., 2007, Tischler et al., 2007, Jacko et al., 2021b]. (a) The compression during the Lower Miocene in the ESB was related to the overall closing of the accretion wedge, where the slope of the subducting plate was about 32°. These are the deformation conditions where compression dominates in the upper part of the crust, and it is manifested in a wider regional context. As the shortening progressed from the north to the south, lateral dextral transpressional movements were generated in the Pieniny Klippen Belt zone, which also generated important structural fault systems in the developing ESB. The progradation process of basins closure caused the ALCAPA to be pushed onto Tisza–Dacia along the Mid-Hungarian fault zone. (b) In the Upper Badenian (Lower Serravallian), the tectonic situation changed. The main cause was a change in the inclination of the subduction plate. The deformation conditions changed where there was an increase in the slab inclination. The upper crust began to be dominated by extension, which accelerated the subsidence of the area north of the MHFZ. This caused roll-back dips, offset by uplifts on the opposite side of the basin (Figure 15). The shortening and thrusting of the MHFZ was transformed into sinistral movements which caused the counterclockwise rotation of the ALCAPA. The rotation of the plate was reduced along the N–S faults of the Hornád fault system, which separated the subducting plate into a western (shallow) and an eastern (steep) segment. (c) The transition from transpression to MHFZ transtension supported the ongoing dynamic subsidence of ESB. Syn-sedimentary oblique movements at faults parallel to the basin axis (NW–SE) are offset by the emergence of oppositely oriented growth faults/relay ramps. Abbreviations: Outer Western Carpathian (OWC), Pieniny Klippen Belt (PKB), Inner Western Carpathian (IWC), Iňačovce–Kritchevo Unit (IKU), East Slovakian Basin (ESB), Hornád Fault (HF), Trebišov Fault (TF), Diojenö Fault (DF), Albinov Fault (AF), Mid-Hungarian Fault Zone (MHFZ).

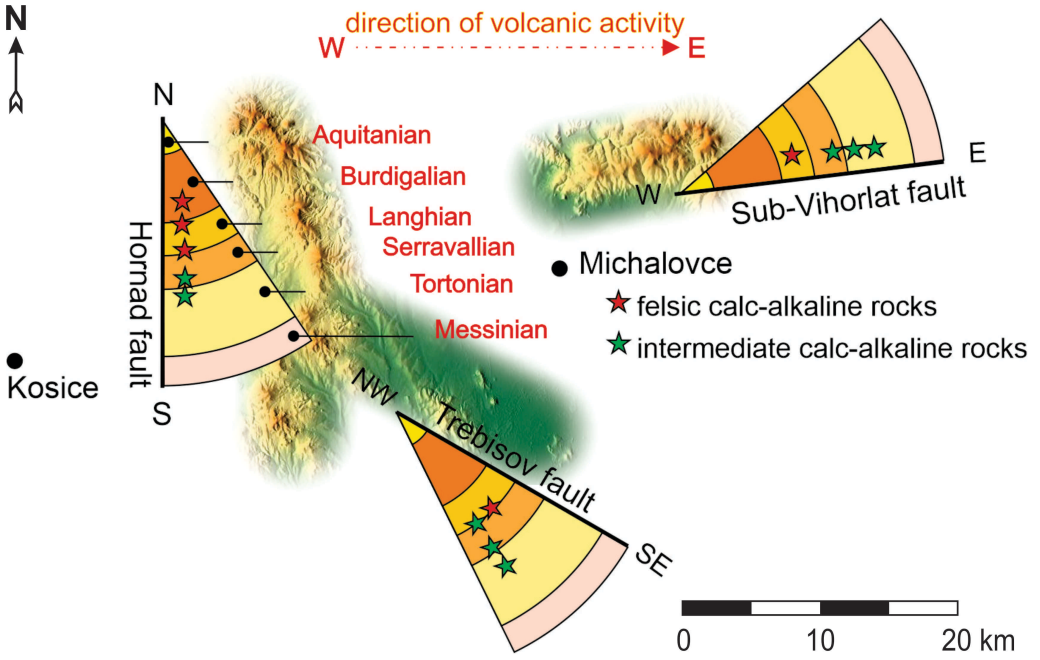

Figure 14. Timeline of volcanic activity linked to morphologically and tectonically active fault system of the ESB. The volcanic sequence is marked by stars (red, green) and movement from west to east is parallel to the oblique subduction [sensu Pécskay et al., 2006].

was covered by products of the Vihorlat Mts. Volcanic Chain. The chain consists of 5 large pyroxene andesite stratovolcanoes (12.5–9.1 Ma) with pyroclastic rocks, dikes and sills.

The volcanic evolution of the ESB occurred alongside sedimentary, tectonic and geodynamic events which were important in the Middle Miocene [Tomek et al., 1987, Kováč et al., 1989, 1993, 1994, Marko et al., 1990, 1991, Fodor et al., 1999]. Crustal bending and later crustal breaching was recorded not only in the sediments, but also in the volcanic activity, and subduction. These relationships emphasize the observable volcanic migration, not just geographically, but also in the magmatic composition, from felsic to intermediate alkaline rocks. The last stage of volcanism is linked to the Vihorlat Mts. Chain. Here, the melting of steeply inclined crust created stratovolcanoes on the border with the accretionary wedge, this is linked to slab break-off.

5.2. *Geodynamic aspects*

The geodynamic factors in the subduction zone are linked to back-arc extension and the rollback of the subduction hinge. Experiments [Faccenna et al., 2001, Schellart et al., 2003] have shown that rapid hinge rollback is caused by an increase in buoyancy forces and by the steepening of the subducting slab [Hall et al., 2003]. The total dynamic conditions for the subducting slab are defined as a combination of: (a) surface kinematics, (b) properties of the descending slab and the (c) effect of lateral mantle flow on the subducting slab [Sdrolias and Müller, 2006].

The ESB evolution reflects specific conditions which are related to the asymmetrical spreading of the Pannonian basin, which was predominantly opened towards the NE. This opening was made possible by block movement. The block movements caused the rotation of microplates, which were linked to transpression along the MHFZ. This process involved marginal peripheral areas, that were relatively tectonically autonomous, and which were accelerated by subduction and slab inclination changes.

Relay ramps are a good “litmus test” for tracking geodynamic processes in an extensional environment. Their structural evolution sensitively records

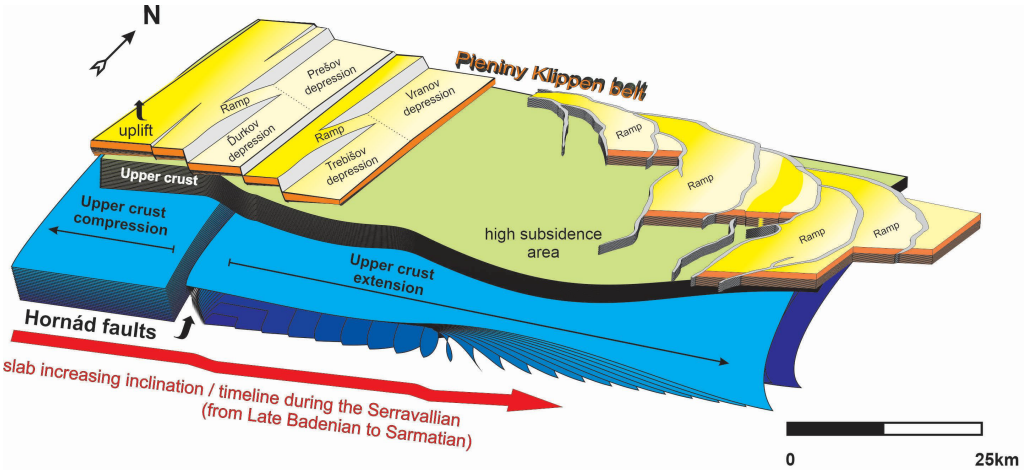

Figure 15. Spatial timeline and architectural model. A view of the interaction between upper crust forces which opened the Eastern Slovak Basin, and ramp structures which developed as the result of gradual increases in slab inclination, from west to east.

conditional changes and sedimentation. Current published knowledge from the ESB has so far not included relay ramp structures, or their importance for the tectonic structure and basin evolution. New seismic data, models, and new deep boreholes for hydrocarbon and geothermal prospection show the importance of relay ramps. Even though their development mainly took place in the Middle Miocene, they occur in the tectonic record younger periods, even up until the present.

The development of the relay ramp is closely tied to slab geometry (Figure 15), which has been often discussed [Jolivet et al., 2013, Lallemand et al., 2005, Papanikolaou and Royden, 2007, Taymaz et al., 2004]. In the Middle Miocene slab inclination start to change with direct effect to increasing sedimentation (from Langhian to Serravallian, 14–11 Ma). If we correlate the slab dip changes to the present slab dips of the back-arc basins, we cannot find large differences.

Basins which are dominated by back-arc spreading have steep dips larger than 51°. The steep slabs were observed in more than 42% of the peripheral basins [Lallemand et al., 2005]. These are acceptable tectonic conditions for relay ramp development. A good example is from the Aegean back-arc of the Hellenic subduction zone. This zone has a complex tectonic history, which describes the geometry of slab retreat and fragmentation [Jolivet et al., 2013, Papanikolaou and Royden, 2007, Taymaz et al., 2004]. The relay ramps were formed paralel to major faults and later coincided with steepening of the slab. Later they were modified into connected bridges between transfer faults and were used as pathways for magma intrusion [Hooft et al., 2017]. Active seismicity and relay ramp geometry in the Aegean basin are related to each other. The parts of the fault with the highest normal fault displacement rate are seismically active, whereas the opposite arm is relatively stable. This example is also applicable in the ESB. The high subsidence area of the ESB is concentrated on the SE edge of the basin which is currently the lowest point (98 m.a.s.l.) in the whole of the Western Carpathians. This same point, where all three main fault systems converge (NW–SE, N–S and NE–SW), is associated with the last earthquake from October 2023 $M = 5.1$.

Lateral paleomantle flow on the subducting slab is difficult to determine in the post active areas. However, it is possible to interpret it from the paleoreconstruction of sedimentary and volcanic activity, and their relationship to the Moho. Further relationships arise when one compares the locations of the ESB's fault systems with the thicknesses of the Moho depth map isolines [Bielik et al., 2010, Janik et al., 2011]. The Darnó Fault Zone follows an approximately 27 km Moho depth isoline and bounds the southwestern limb of overheated NE–SW Moho antiform structure. This structure continues towards the NE section of

the ESB and is parallel to the highest thermal flow area of the Pannonian basin. The Slanské Mts. located directly along the N–S axial zone of the dome continuously preserves both mentioned courses of the Moho dome. The semiplastic Moho model formed during active rifting conditions was supported by simultaneously increasing thermal flow, which resulted in the undulated shape of the thinned Moho. The spatial relationships between the surface thermal flow isolines, the main faults, and the Slanské Mts. neovolcanic chain connect the apical parts of undulated Moho morphology in the East Slovakia region. This clearly indicates that these structures are mutually interconnected. These relationships are especially sensible in the Eastern Slovak Basin territory. Here, maximal thermal flow isolines (which are linked to the parts of the region with the thinnest crust) are spatially controlled by two NW–SE and N–S dominating fault sets. It is worth mentioning that the max.—e.g., 120 °C thermal flow isoline, located at the connecting point of the N–S and the NE–SW faults, has an opposite—NW–SE course [Jacko et al., 2021a].

6. Conclusions

The opening of a depositional space at the collision zone boundary, to accommodate the Eastern Slovak Basin, was generated by the closure of an accretionary wedge. The wedge formed a transpressional environment which generated a boundary wrench, and tensile compensation structures. The structures were later used as pilot faults for basin formation, which were related to the subsequent deformation processes.

The transition from upper crust compression to upper crust extension accelerated tilting progradation. The increased slab inclination generated fractures which were parallel to the collision zone, and which were perpendicular to the basin opening direction. This significantly influenced the basin's subsidence, shape, and the migration of the depositional environment. The core breakage, caused by the transform fault parallel with Hornád Fault System, was a crucial moment for the later evolution of the basin. The N–S fault direction is connected with a wedge of antithetic reader shears. Along the fault linked to slab inclination volcanism, relay ramp development, depositional changes, rapid and deep subsidence of the basin (up to 8 km) are observed.

The deep subsidence, up to 60 km in length, would not have been possible without the existence of the relay ramp system. The four evolutionary stages were controlled by crust mechanical conditions, which were supported by thermal heating. The relay ramps created an effective system of listric normal faults, where negative movement on one side of the fault was compensated by uplift on the opposite side of the fault (close to the accretionary wedge). This arm fault mechanism is well-preserved up until now, as evidenced by the earthquake from October 2023 $M = 5.1$.

Relay ramp structural zonality in the basin is important for the understanding of deep hydrocarbon and geothermal deposits.

Declaration of interests

The authors do not work for, advise, own shares in, or receive funds from any organization that could benefit from this article, and have declared no affiliations other than their research organizations.

Funding

This research was funded by the Slovak Grant Agency VEGA, grants 1/0585/20.

References

Bada, G., Horváth, F., Cloetingh, S., Conbletz, D. D., and Tóth, T. (2001). Role of topography-induced gravitational stresses in basin inversion. The case study of the Pannonian Basin. *Tectonics*, 20(3), 343–363.

Bada, G., Horváth, F., Dövényi, P., Szafián, P., Windhoffer, G., and Cloetingh, S. (2007). Present-day stress field and tectonic inversion in the Pannonian basin. *Glob. Planet. Chang.*, 58, 165–180.

Bastesen, E. and Rotevatn, A. (2012). Evolution and structural style of relay zones in layered limestone-shale sequences: Insights from the Hammam Faraun Fault Block, Suez Rift, Egypt. *J. Geol. Soc. Lond.*, 169, 477–488.

Bielik, M., Alasonati-Tašárová, Z., Zeyen, H., Dérerová, J., Afonso, J. C., and Csicsay, K. (2010). Improved geophysical image of the Carpathian–Pannonian basin region. *Acta Geod. Geoph. Hung.*, 45(3), 284–298.

Brown, A. R. (1991). *Interpretation of Three-Dimensional Seismic Data*. AAPG, Tulsa, Oklahoma, 3rd edition.

Cloetingh, S., Bada, G., Matenco, L., Lankreijer, A., Horvath, F., and Dinu, C. (2006). Modes of basin (de)formation, lithospheric strength and vertical motions in the Pannonian–Carpathian system: inferences from thermomechanical modelling. *Geol. Soc. Lond. Mem.*, 32, 207–221.

Cloetingh, S., Matenco, L., Bada, G., Dinu, C., and Mocanu, V. (2005). The evolution of the Carpathians–Pannonian system: Interaction between neotectonics, deep structure, polyphase orogeny sedimentary basins in a source to sink natural laboratory. *Tectonophysics*, 410(1–4), 1–14.

Corfield, S. and Sharp, I. R. (2000). Structural style and stratigraphic architecture of fault propagation folding in extensional settings: a seismic example from the Smørbukk area, Halten Terrace, Mid Norway. *Basin Res.*, 12, 329–341.

Cowie, P., Gupta, S., and Dawers, N. H. (2000). Implications of fault array evolution for synrift depocentre development: insights from a numerical fault growth model. *Basin Res.*, 12, 241–261.

Csontos, L. (1995). Tertiary tectonic evolution of the Intra-Carpathian area: a review. In Downes, H. and Vaselli, O., editors, *Neogene and Related Magmatism in the Carpatho-Pannonian Region*, volume 7 of *Acta Vulcanologica*, pages 1–13. National Volcanic Group of Italy, Pisa.

Csontos, L. and Nagymarosy, A. (1998). The Mid-Hungarian line: a zone of repeated tectonic inversions. *Tectonophysics*, 297, 51–71.

Csontos, L., Nagymarosy, A., Horváth, F., and Kováč, M. (1992). Tertiary tectonic evolution of the Intra-Carpathian area: A model. *Tectonophysics*, 208(1–3), 221–241.

Csontos, L. and Vörös, A. (2004). Mesozoic plate tectonic reconstruction of the Carpathian region. *Palaeogeogr. Palaeoclimatol. Palaeoecol.*, 210, 1–56.

Faccenna, C., Becker, T. W., Lucente, F. P., Jolivet, L., and Rossetti, F. (2001). History of subduction and back-arc extension in the Central Mediterranean. *Geophys. J. Int.*, 145, 809–820.

Fodor, L. (1995). From transpression to transtension: Oligocene-Miocene structural evolution of the Vienna basin and the East Alpine-Western Carpathian junction. *Tectonophysics*, 242(1–2), 151–182.

Fodor, L., Csontos, L., Bada, G., Györfi, I., and Benkovics, L. (1999). Cenozoic tectonic evolution of the Pannonian basin system and neighbouring orogens: a new synthesis of paleostress data. In Durand, B., Jolivet, L., Horváth, F., and Séranne, M., editors, *The Mediterranean Basins: Cenozoic Extension within the Alpine Orogen*, Geological Society, London, Special Publications 156, pages 295–334. Geological Society of London.

Fodor, L., Jelen, B., Márton, E., Skaberne, D., Car, J., and Vrabec, M. (1998). Miocene-Pliocene evolution of the Slovenian Periadriatic fault: Implications for Alpine Carpathian extrusion models. *Tectonics*, 17, 690–709.

Fodor, L., Radócz, G., Sztanó, O., Koroknai, B., Csontos, L., and Harangi, S. (2005). Postconference excursion: tectonics, sedimentation and magmatism along the Darnó Zone. *GeoLines*, 19, 142–162.

Fossen, H. and Rotevatn, A. (2016). Fault linkage and relay structures in extensional settings—a review. *Earth-Sci. Rev.*, 154, 14–28.

Fričovský, B., Jacko, S., Chytilová, M., and Tometz, L. (2012). Geothermal energy of Slovakia—CO_2 emissions reduction contribution potential (background study for conservative and non-conservative approach). *Acta Montan. Slovaca*, 17(4), 290–299.

Gawthorpe, R. L. and Leeder, M. R. (2000). Tectono-sedimentary evolution of active extensional basins. *Basin Res.*, 12, 195–218.

Gawthorpe, R. L., Sharp, I., Underhill, J. R., and Gupta, S. (1997). Linked sequence stratigraphy and structural evolution of propagating normal faults. *Geology*, 25(9), 795–798.

Giba, M., Walsh, J. J., and Nicol, A. (2012). Segmentation and growth of an obliquely reactivated normal fault. *J. Struct. Geol.*, 39, 253–267.

Ginger, D. C., Ardjakusumah, W. O., Hedley, R. J., and Pothecary, J. (1993). Inversion history of the West Natuna basin: examples from Cumi-Cumi PSC. In *Proceedings Indonesian Petroleum Association*, volume 22, pages 635–658. Indonesian Petroleum Association, Jakarta.

Hall, C. E., Gurnis, M., Sdrolias, M., Lavier, L. L., and Müller, R. D. (2003). Catastrophic initiation of subduction following forced convergence across fracture zones. *Earth Planet. Sci. Lett.*, 212, 15–30.

Hall, R. (2002). Cenozoic geological and plate tectonic evolution of SE Asia and the SW Pacific:

computer-based reconstructions, model and animations. *J. Asian Earth Sci.*, 20, 353–431.

Hamblin, W. K. (1965). Origin of "reverse drag" on the downthrown side of normal faults. *Bull. Geol. Soc. Am.*, 16, 1154–1164.

Haq, U., Hardenbol, J., and Vail, P. R. (1987). Chronology of fluctuating sea levels since the Triassic. *Science*, 235, 1156–1167.

Higgs, R. (1999). Gravity anomalies, subsidence history and the tectonic evolution of the Malay and Penyu Basins (offshore Peninsular Malaysia)—discussion. *Basin Res.*, 11(3), 285–290.

Hlavatá, J. and Kováč, M. (2010). Change of sedimentary record as a consequence of changes in depth and dynamics of depositional environment (East Slovakian Basin, Middle Miocene). *Acta Geol. Slovaca*, 2(1), 37–46.

Hooft, E. E., Nomikou, P., Toomey, D. R., Lampridou, D., Getz, C., Christopoulou, M., O'Hara, D., Arnoux, G. M., Bodmer, M., Gray, M., Heath, B. A., and VanderBeek, B. P. (2017). Backarc tectonism, volcanism, and mass wasting shape seafloor morphology in the Santorini-Christiana-Amorgos region of the Hellenic Volcanic Arc. *Tectonophysics*, 712–713, 396–414.

Horváth, F., Bada, G., Szafián, P., Tari, G., Ádám, A., and Cloetingh, S. (2006). Formation and deformation of the Pannonian basin: Constraints from observational data. In Gee, D. G. and Stephenson, R. A., editors, *European Lithosphere Dynamics*, Geological Society, London, Memoirs 32, pages 191–206. Geological Society of London.

Horváth, F. and Cloetingh, S. (1996). Stress-induced late-stage subsidence anomalies in the Pannonian basin. *Tectonophysics*, 266, 287–300.

Horváth, F., Musitz, B., Balázs, A., Végh, A., Uhrine, A., Nádor, A., Koroknai, B., Pap, N., Tótha, T., and Wórum, G. (2015). Evolution of the Pannonian basin and its geothermal resources. *Geothermics*, 53, 328–352.

Hrušecký, I., Jacko, S., Janočko, J., Kotulová, J., Karoli, S., Zlinská, A., Hurai, V., Biroň, A., and Zuberec, J. (2000). Hydrocarbon potential of East Slovakian Neogene basin and adjacent flysch belt area. *Geologické práce, Správy*, 104, 1–42.

Huggins, P., Watterson, J., Walsh, J. J., and Childs, C. (1995). Relay zone geometry and displacement transfer between normal faults recorded in coalmine plans. *J. Struct. Geol.*, 17(12), 1741–1755.

Jacko, S., Farkašovský, R., Ďuriška, I., Ščerbáková, B., and Bátorová, K. (2021a). Critical tectonic limits for geothermal aquifer use: Case study from the East Slovakian basin rim. *Resources*, 10(4), article no. 31.

Jacko, S., Fričovský, B., Pachocká, K., and Vranovská, A. (2014). Stationary reverse temperature modeling and geothermal resources callibration for the Košice depression (Eastern Slovakia). *Technika poszukiwań geologicznych : Geotermia, Zrównowazony rozvój*, 53(1), 3–25.

Jacko, S., Jacko sen, S., Labant, S., Bátorová, K., Farkašovský, R., and Ščerbáková, B. (2021b). Structural contraints of neotectonic activity in the eastern part of the Western Carpathians orogenic wedge. *Quat. Int.*, 585, 27–43.

Janik, T., Grad, M., Guterch, A., Vozár, J., Bielik, M., Vozárová, A., Hegedűs, E., Kovács, C. A., and Kovács, I. (2011). CELEBRATION 2000 Working group crustal structure of the Western Carpathians and Pannonian basin system: seismic models from CELEBRATION 2000 data and geological implication. *J. Geodyn.*, 52(2), 97–113.

Janočko, J. (1990). Sedimentation environment of the Varhaňovce gravels in the northern part of the Košická kotlina basin (Eastern Slovakia). *Miner. Slovaca*, 22, 539–546.

Janočko, J. (1993). Development of a braided delta depositional system—Lower Sarmatian, Neogene East Slovakian Basin. In Vass, D., editor, *Sedimentological and Paleogeographical Analysis of the East Slovakian Basin*, pages 1–16. GUDŠ, Bratislava.

Janočko, J. (1996). Sediments in faces of small deltas in the Eastern Slovakian basin. *Geologické práce, Správy*, 101, 25–26.

Janočko, J., Pereszlenyi, M., Vass, D., Bezak, V., Jacko Jr, S., Jacko, S., Kohut, M., Polak, M., and Mello, J. (2006). Geology and hydrocarbon resources of the Inner Western Carpathians, Slovakia, and Poland. In Golonka, J. and Picha, F. J., editors, *The Carpathians and their Foreland: Geology and Hydrocarbon Resources*, AAPG Memoir 84, pages 569–603. AAPG, Tulsa, Oklahoma.

Jardine, E. (1997). Dual petroleum systems governing the prolific Pattani Basin, offshore Thailand. In Howes, J. V. C. and Noble, R. A., editors, *Proceedings of the International Conference on Petroleum Systems of SE Asia and Australia*, pages 351–363. Indonesian Petroleum Association, Jakarta.

Jolivet, L., Faccenna, C., Huet, B., Labrousse, L., Le Pourhiet, L., Lacombe, O., Lecomte, E., Burov, E., Denèle, Y., Brun, J. P., Philippon, M., Paul, A., Salaün, G., Karabulut, H., Piromallo, C., Monié, P., Gueydan, F., Okay, A. I., Oberhänsli, R., Pourteau, A., Augier, R., Gadenne, L., and Driussi, O. (2013). Aegean tectonics: progressive strain localisation, slab tearing and trench retreat. *Tectonophysics*, 597–598, 1–33.

Konečný, V., Kováč, M., Lexa, J., and Šefara, J. (2002). Neogene evolution of the Carpatho-Pannonian region: an interplay of subduction and back-arc uprise in the mantle. *EGU St. Mueller Spec. Publ. Ser.*, 1, 105–123.

Kováč, M., Baráth, I., Holický, I., Marko, F., and Túnyi, I. (1989). Basin opening in the Lower Miocene strike-slip zone in the SW part of the Western Carpatbians. *Geol. Carpathica*, 40, 37–62.

Kováč, M., Bielik, M., Lexa, J., Pereszlényi, M., Šefara, J., Túnyi, I., and Vass, D. (1997). The Western Carpathian intramountane basins. In Grecula, P., editor, *Geological Evolution of the Western Carpathians*, Monograph, pages 43–65. Mineralia Slovaca, Bratislava.

Kováč, M., Král', J., Márton, E., Plašienka, D., and Uher, P. (1994). Alpine uplift history of the Central Western Carpathians: geochronological, paleomagnetic, sedimentary and structural data. *Geol. Carpathica*, 45, 83–96.

Kováč, M., Lexa, J., Konečný, V., and Šefara, J. (2002). Geodynamic evolution of the Carpathian–Pannonian region during the Neogene. *Geol. Carpathica*, 53(special issue), 1–2.

Kováč, M., Márton, E., Kl'učiar, T., and Vojtko, R. (2018). Miocene basin opening in relation to the north-eastward tectonic extrusion of the ALCAPA Mega-Unit. *Geol. Carpathica*, 69(3), 254–263.

Kováč, M., Márton, E., Oszczypko, N., Vojtko, R., Hók, J., Králiková, S., Plašienka, D., Klučiar, T., Hudáčková, N., and Oszczypko-Clowes, M. (2017). Neogene palaeogeography and basin evolution of the Western Carpathians, Northern Pannonian domain and adjoining areas. *Glob. Planet. Change*, 155, 133–154.

Kováč, M., Nagymarosy, A., Oszczypko, N., Slaczka, A., Csontos, L., Marunteanu, M., Matenco, L., and Márton, M. (1998). Palinspastic reconstruction of the Carpathian–Pannonian region during the Miocene. In Rakús, M., editor, *Development of the Western Carpathians Geodynamic*, pages 189–217. Geological Survey of Slovak Republick, Bratislava.

Kováč, M., Nagymarosy, A., Soták, J., and Šutovská, K. (1993). Late Tertiary paleogeographic evolution of the Western Carpathians. *Tectonophysics*, 226, 401–415.

Kováč, M., Plašienka, D., Soták, J., Vojtko, R., Oszczypko, N., Less, G., Ćosović, V., Fügenschuh, B., and Králiková, S. (2016). Paleogene palaeogeography and basin evolution of the Western Carpathians, Northern Pannonian domain and adjoining areas. *Glob. Planet. Change*, 140, 9–27.

Lallemand, S., Heuret, A., and Boutelier, D. (2005). On the relationships between slab dip, back-arc stress, upper plate absolute motion, and crustal nature in subduction zones. *Geochem. Geophys. Geosyst.*, 6(9), article no. Q09006.

Lexa, J. and Konečný, V. (1998). Geodynamic aspects of the Neogene to Quaternary volcanism. In Rakús, M., editor, *Geodynamic Development of the Western Carpathians*, pages 219–240. Geological Survey of Slovak Republick, Bratislava.

Lexa, J., Seghedi, I., Németh, K., Szakács, A., Konecný, V., Pécskay, Z., Fülöp, A., and Kovacs, M. (2010). Neogene-quaternary volcanic forms in the Carpathian–Pannonian region: a review. *Cent. Eur. J. Geosci.*, 2(3), 207–270.

Madon, M. B. and Watts, A. B. (1998). Gravity anomalies subsidence history and the tectonic evolution of the Malay and Penyu Basins (offshore Peninsular Malaysia). *Basin Res.*, 10, 375–392.

Marko, F., Fodor, L., and Kováč, M. (1991). Miocene strike-slip faulting and block rotation in Brezovské Karpaty Mts. (Western Carpathians). *Miner. Slovaca*, 23, 189–200.

Marko, F., Kováč, M., Fodor, L., and Šutovská, K. (1990). Deformations and kinematics of a Miocene stear zone in the northern part of the Little Carpathians (Buková Furrow, Hrabník Formation). *Miner. Slovaca*, 22, 399–410.

Márton, E. (2000). The Tisza Megatectonic Unit in the light of paleomagnetic data. *Acta Geol. Hung.*, 43, 329–343.

Márton, E. and Fodor, L. (2003). Tertiary paleomagnetic results and structural analysis from the Transdanubian Range (Hungary): rotational disintegration of the ALCAPA unit. *Tectonophysics*, 363, 201–224.

Márton, E., Tischler, M., Csontos, L., Fügenschuh, B.,

and Schmid, S. M. (2007). The contact zone between the ALCAPA and Tisza-Dacia megatectonic units of Northern Romania in the light of new paleomagnetic data. *Swiss J. Geosci.*, 100, 109–124.

Matenco, L. and Andriessen, P. (2013). Quantifying the mass transfer from mountain ranges to deposition in sedimentary basins: Source to sink studies in the Danube Basin–Black Sea system. *Glob. Planet. Change*, 103, 1–18.

McClay, K. R. and Ellis, P. G. (1987). Analogue models of extensional fault geometries. *Geol. Soc. Lond. Spec. Publ.*, 28, 109–125.

Minár, J., Bielik, M., Kováč, M., Plašienka, D., Barka, I., Stankovianský, M., and Zeyen, H. (2011). New morphostructural subdivision of the Western Carpathians: An approach integrating geodynamics into targeted morphometric analysis. *Tectonophysics*, 502(1–2), 158–174.

Morley, C. F., Nelson, R. A., Patton, T. L., and Munn, S. G. (1990). Transfer zones in the East African Rift System and their relevance to hydrocarbon exploration in rifts. *AAPG Bull.*, 71, 1234–1253.

Morley, C. K. (1995). Developments in the structural geology of rifts over the last decade and their impact on hydrocarbon exploration. *Geol. Soc. Lond. Spec. Publ.*, 80, 1–32.

Morley, C. K. (2001). Combined escape tectonics and subduction rollback backarc extension: a model for the Tertiary rift basin in Thailand, Malaysia and Laos. *J. Geol. Soc. Lond.*, 158, 461–474.

Müller, R. D., Sdrolias, M., Gaina, C., and Roest, W. R. (2008). Age, spreading rates, and spreading asymmetry of the world's ocean crust. *Geochem. Geophys. Geosyst.*, 9(4), article no. Q04006.

Nemčok, M., Krzywiec, P., Wojtaszek, M., Ludhová, L., Klecker, R. A., Sercombe, W. J., and Coward, M. P. (2006). Tertiary development of the Polish and eastern Slovak parts of the Carpathian accretionary wedge: insights from balanced cross-sections. *Geol. Carpathica*, 57, 355–370.

Neubauer, F., Genser, J., and Handler, R. (2000). The Eastern Alps: result of a two-stage collision process. *Mitt. Österr. Geologischen Gesellschaft*, 92, 117–134.

Oszczypko, N. (1998). The Western Carpathians Foredeep development of the foreland basin in front of acretionary wedge and its burial history (Poland). *Geol. Carpathica*, 49(6), 415–431.

Oszczypko, N. (1999). From remnant oceanic basin to collision-related foreland basin a tentative history of the Outer Western Carpathians. *Geol. Carpathica*, 50(special issue), 161–163.

Oszczypko, N. (2006). Late Jurassic-Miocene evolution of the Outer Carpathian fold-and-thrust belt and its foredeep basin (Western Carpathians, Poland). *Geol. Q.*, 50, 169–194.

Oszczypko, N., Olszewska, B., and Malata, E. (2012). Cretaceous (Aptian/Albian–? Cenomanian) age of "black flysch" and adjacent deposits of the Grajcarek thrust-sheets in the Małe Pieniny Mts. (Pieniny Klippen Belt, Polish Outer Carpathians). *Geol. Q.*, 56, 411–440.

Oszczypko, N. and Oszczypko-Clowes, M. (2006). Evolution of the Magura Basin. In Oszczypko, N., Uchman, A., and Malata, E., editors, *Paleotectonic Evolution of the Outer Carpathian and Pieniny Klippen Belt Basins*, pages 133–164. Geological Institute of Jagellonian University, Krakow.

Pachocka, K., Jacko, S., and Pachocki, M. (2010). *3D Modeling of a Geothermal Reservoir in Eastern Slovakia Area: The Central Part of Kosice Basin*. VDM Verlag, Saarbrücken.

Papanikolaou, D. J. and Royden, L. H. (2007). Disruption of the Hellenic arc: Late Miocene extensional detachment faults and steep Pliocene-Quaternary normal faults—or what happened at Corinth? *Tectonics*, 26, article no. TC5003.

Peacock, D. C. P. and Sanderson, D. J. (1991). Displacements, segment linkage and relay ramps in normal fault zones. *J. Struct. Geol.*, 13, 721–733.

Peacock, D. C. P. and Sanderson, D. J. (1994). Geometry and development of relay ramps in normal fault systems. *AAPG Bull.*, 78, 147–165.

Pécskay, Z., Lexa, J., Szakács, A., Seghedi, I., Balogh, K., Konecny, V., Zelenka, T., Kovacs, M., Póka, T., Fülöp, A., Márton, E., Panatiotu, C., and Cvetkovic, V. (2006). Geochronology of Neogene magmatism in the Carpathian arc and intra-Carpathian area. *Geol. Carpathica*, 57, 511–530.

Pickering, J. L., Goodbred, S. L., Reitz, M. D., Hartzog, T. R., Mondal, D. R., and Hossain, M. S. (2014). Late Quaternary sedimentary record and Holocene channel avulsions of the Jamuna and Old Brahmaputra River valleys in the upper Bengal delta plain. *Geomorphology*, 227, 127–136.

Ratschbacher, L., Frisch, W., Linzer, H.-G., and Merle, O. (1991). Lateral extrusion in the Eastern Alps; Part 2, Structural analysis. *Tectonics*, 10, 257–271.

Ratschbacher, L., Linzer, H. G., and Moser, F. (1993). Cretaceous to Miocene thrusting and wrenching along the Central South Carpathians due to a corner effect during collision and orocline formation. *Tectonics*, 12, 855–873.

Rauch, M. (2013). The Oligocene-Miocene tectonic evolution of the northern Outer Carpathian fold- and thrust belt: insights from compression-and-rotation analogue modelling experiments. *Geol. Mag.*, 150, 1062–1084.

Reed, K., Janočko, J., Vass, D., and Gibson Jr, M. (1992). A sedimentological and petrographic investigation of the Nizny Caj K-8 well. *Miner. Slovaca*, 24, 219–226.

Řeřicha, M. (1992). The Upper Badenian delta in the Eastern Slovakian Neogene Basin. *Miner. Slovaca*, 24, 63–68.

Rotevatn, A. and Bastesen, E. (2012). Fault linkage and damage zone architecture in tight carbonate rocks in the Suez Rift (Egypt): implications for permeability structure along segmented normal faults. In Spence, G. H., Redfern, J., Aguilera, R., Bevan, T. G., Cosgrove, J. W., Couples, G. D., and Daniel, J.-M., editors, *Advances in the Study of Fractured Reservoirs*, Geological Society, London, Special Publications 374, pages 79–95. Geological Society of London.

Rotevatn, A. and Jackson, C. A.-L. (2014). 3D structure and evolution of folds during normal fault dip linkage. *J. Geol. Soc.*, 171(6), 821–829.

Royden, L. H. (1988). Late cenozoic tectonics of the Pannonian basin system. In Royden, L. H. and Horvath, F., editors, *The Pannonian Basin; A Study in Basin Evolution*, AAPG Memoir 45, pages 27–48. American Association of Petroleum Geologists, Tulsa, Oklahoma.

Sály, B., Janočko, J., Jacko, S., Jureňa, V., and Hlavaty, I. (2006). New results in the mature East Slovakian basin based on 3D and 2D seismic data interpretation and sequence stratigraphy. In *Proceedings of Society of Petroleum Engineers, 68th European Association of Geoscientists and Engineers Conference and Exhibition, Incorporating SPE EUROPEC 2006, EAGE 2006: Opportunities in Mature Areas, June 2006*, pages 2712–2716. European Association of Geoscientists & Engineers, Bunnik, Utrecht.

Schellart, W. P., Jessell, M. W., and Lister, G. S. (2003). Asymmetric deformation in the backarc region of the Kuril arc, northwest Pacific: New insights from analogue modeling. *Tectonics*, 22(5), article no. 1047.

Schlische, R. W. (1995). Geometry and origin of fault-related folds in extensional settings. *AAPG Bull.*, 79, 1661–1678.

Schmid, S. M., Bernoulli, D., Fügenschuh, B., Matenco, L., Schuster, R., Schefer, S., Tischler, M., and Ustaszewski, K. (2008). The Alpine-Carpathian-Dinaridic orogenic system: correlation and evolution of tectonic units. *Swiss J. Geosci.*, 101, 139–183.

Sdrolias, M. and Müller, R. D. (2006). Controls on back-arc basin formation. *Geochem. Geophys. Geosyst.*, 7(4), article no. Q04016.

Seghedi, I. and Downes, H. (2011). Geochemistry and tectonic development of Cenozoic magmatism in the Carpathian–Pannonian region. *Gondwana Res.*, 20, 655–672.

Serck, C. S. and Braathen, A. (2018). Extensional fault and fold growth: Impact on accommodation evolution and sedimentary infill. *Basin Res.*, 31, 967–990.

Sharp, I. R., Gawthorpe, R. L., Underhill, J. R., and Gupta, S. (2000). Fault propagation folding in extensional settings: Examples of structural style and synrift sedimentary response from the Suez rift, Sinai, Egypt. *Bull. Geol. Soc. Am.*, 112, 1877–1899.

Shepherd, M. (2009). Meandering fluvial reservoirs. In Shepherd, M., editor, *Oil Field Production Geology*, pages 262–272. Tulsa, Oklahoma, 1st edition.

Soliva, R. and Benedicto, A. (2004). A linkage criterion for segmented normal faults. *J. Struct. Geol.*, 26(12), 2251–2267.

Soliva, R. and Schultz, R. A. (2008). Distributed and localized faulting in extensional settings: insight from the North Ethiopian Rift–Afar transition area. *Tectonics*, 27, 1–19.

Sperner, B. and The CRC 461 Team (2005). Monitoring of slab detachment in the Carpathians. In Wenzel, F., editor, *Perspectives in Modern Seismology*, volume 105 of *Lecture Notes in Earth Sciences*, pages 187–202. Springer, Berlin.

Taymaz, T., Westaway, R., and Reilinger, R. (2004). Active faulting and crustal deformation in the Eastern Mediterranean region. *Tectonophysics*, 391, 1–9.

Tischler, M., Gröger, H. R., Fügenschuh, B., and Schmid, S. M. (2007). Miocene tectonics of the Maramures area (Northern Romania): implications for the Mid-Hungarian fault zone. *Int. J. Earth. Sci.*, 96, 473–496.

Tjia, H. D. and Liew, K. K. (1996). Changes in tectonic stress field in northern Sunda Shelf Basins. In Hall, R. and Blundell, D. J., editors, *Tectonic Evolution of SE Asia*, Geological Society, London, Special Publications, pages 291–306. Geological Society of London.

Tomek, Č., Dvořákova, L., and Ibrmajer, I. (1987). Crustal profiles of active continental collisional belt: Czechoslovak deep siesmic profiling in the West Carpathians. *Geophys. J. Int.*, 89, 383–388.

Trudgill, B. and Cartwright, J. (1994). Relay-ramp forms and normal-fault linkages, Canyonlands National Park, Utah. *Geol. Soc. Am. Bull.*, 106, 1143–1157.

Ustaszewski, K., Kounov, A., Schmid, S. M., Schaltegger, U., Krenn, E., Frank, W., and Fügenschuh, B. (2010). Evolution of the Adria-Europe plate boundary in the northern Dinarides: from continent-continent collision to back-arc extension. *Tectonics*, 29, 1–34.

Ustaszewski, K., Schmid, S. M., Fügenschuh, B., Tischler, M., Kissling, E., and Spakman, W. (2008). A map-view restoration of the Alpine-Carpathian-Dinaridic system for the Early Miocene. *Swiss J. Geosci.*, 101(1), 273–294.

Van Gelder, I. E., Willingshofer, E., Sokoutis, D., and Cloething, S. A. P. L. (2017). The interplay between subduction and lateral extrusion: A case study for the European Eastern Alps based on analogue models. *Earth Planet. Sci. Lett.*, 472, 82–94.

Vass, D., Elečko, M., Janočko, J., Karoli, S., Pereszlenyi, M., Slávik, J., and Kaličiak, M. (2000). Paleogeography of the East–Slovakian basin. *Slov. Geol. Mag.*, 6, 377–407.

Vendeville, B. and Cobbold, P. R. (1988). How normal faulting and sedimentation interact to produce listric fault profiles and stratigraphic wedges. *J. Struct. Geol.*, 10, 649–659.

Walsh, J. J., Bailey, W. R., Childs, C., Nicol, A., and Bonson, C. G. (2003). Formation of segmented normal faults: a 3-D perspective. *J. Struct. Geol.*, 25(8), 1251–1262.

Watcharanantakal, R. and Morley, C. K. (2000). Syn-rift and post rift modelling of the Pattani Basin. Thailand: evidence for ramp-flat detachment. *Mar. Petrol. Geol.*, 17, 937–958.

Withjack, M. O., Schlische, R. W., and Olsen, P. E. (2002). Rift-basin structure and its influence on sedimentary systems. Rift-basin structure and its influence on sedimentary systems. *Soc. Sediment. Geol. Spec. Public.*, 73, 57–58.

Wortel, M. J. R. and Spakman, W. (2000). Subduction and slab detachment in the Mediterranean-Carpathian region. *Science*, 290, 1910–1917.

Wu, J. E., McClay, K., and Frankowicz, E. (2015). Niger Delta gravity-driven deformation above the relict Chain and Charcot oceanic fracture zones, Gulf of Guinea: insights from analogue models. *Mar. Pet. Geol.*, 65, 43–62.

Xu, S., Nieto-Samaniego, Alaniz-Álvarez, S. A., and Cerca-Martínez, L. M. (2011). Structural analysis of a relay ramp in the Querétaro graben, central Mexico: Implications for relay ramp development. *Rev. Mex. Cienc. Geol.*, 28(2), 275–289.

Žec, B., Kaličiak, M., Konečný, V., Lexa, J., Jacko, S., Baňacký, V., Karoli, S., Potfaj, M., Rakús, M., Petro, Ľ., Spišák, Z., Bodnár, J., Jetel, J., Boorová, D., and Zlinská, A. (1997). *Explanation to Geological Map of the Vihorlatské Vrchy Mts. and Humenské Vrchy Mts., Scale 1:50,000.* Geological Survey of Slovak Republick, Bratislava. (in Slovak with English summary).